



Research article

Is aromatic plants environmental health engineering (APEHE) a leverage point of the earth system?

MengYu Lu

HEFEI XIAODOUKOU HEALTH TECH CO LTD, China

A B S T R A C T

It is important to note that every ecological niche in an ecosystem is significant. This study aims to assess the importance of medicinal and aromatic plants (MAPs) in the ecosystem from multiple perspectives. A primary model of Aromatic Plants Environmental Health Engineering (APEHE) has been designed and constructed. The APEHE system was used to collect aerosol compounds, and it was experimentally verified that these compounds have the potential to impact human health by binding to AKT1 as the primary target, and MMP9 and TLR4 as secondary targets. These compounds may indirectly affect human immunity by reversing drug resistance in drug-resistant bacteria in the nasal cavity. This is mainly achieved through combined mutations in *sdhA*, *scrA*, and *PEP*. Our findings are based on Network pharmacology and molecular binding, drug-resistance rescue experiments, as well as combined transcriptomics and metabolomics experiments. It is suggested that APEHE may have direct or indirect effects on human health.

We demonstrate APEHE's numerous potential benefits, such as attenuation and elimination of airborne microorganisms in the environment, enhancing carbon and nitrogen storage in terrestrial ecosystems, promoting the formation of low-level clouds and strengthening the virtuous cycle of Earth's ecosystems. APEHE also supports the development of transdisciplinary technologies, including terpene energy production. It facilitates the creation of a sustainable circular economy and provides additional economic advantages through urban optimisation, as well as fresh insights into areas such as the habitability of other planets. APEHE has the potential to serve as a leverage point for the Earth system. We have created a new research direction.

1. Background

We all know that the earth is a whole system, and we also know the disadvantages of environmental damage and air pollution, such as the effects of the excessive warming of the earth.

In Earth's ecosystems, plants have been very important ecological nodes, and in addition to primary metabolites, plants produce secondary metabolites (SM) to play various roles in response to the changing environment, growth and development [1,2].

Historical records show that in ancient times, aromatic plants were frequently used to combat epidemics, including the plague.

In China, for thousands of years, traditional Chinese medicine has been "aromatic avoid filth, aromatic removal of turbid evils" concept. However, due to the limitation of ancient scientific research, agricultural technology and urban living, afforestation structure of City, aromatic plants natural growth in the environment has not been enough attention. Their benefits have only been considered in relation to human body damage and sickness. Research has shown that the volatile fat-soluble small molecule compounds in aromatic plants secondary metabolites can cross the blood-brain barrier and have the therapeutic effect of reducing inflammation and antioxidants [3–5]. The possible pathway is through the olfactory epithelium through the central nervous system (CNS) and the olfactory bulb and the respiratory system as a sedative or stimulator to absorb molecules into the blood or circulation [5]. In the decocting process of traditional Chinese medicine, these small molecule compounds are easily volatile into the air, and if only used as a

E-mail address: mengyulu@apehe.com.

<https://doi.org/10.1016/j.heliyon.2024.e30322>

Received 10 January 2024; Received in revised form 30 March 2024; Accepted 23 April 2024

Available online 3 May 2024

2405-8440/© 2024 The Author(s). Published by Elsevier Ltd. This is an open access article under the CC BY-NC-ND license (<http://creativecommons.org/licenses/by-nc-nd/4.0/>).

decoction, many effective volatiles will be lost.

Traditional Chinese medicine has many different methods in the processing and use of medicinal materials. During the epidemic period, burning and cooking of medicinal and aromatic plants (MAPs) volatile compounds are used to hinder the spread of the disease. Although from the past in the prevention and treatment of infectious diseases we cannot understand the aromatic volatile in what is the role of outbreaks, but the Chinese traditional culture as the 24 solar terms discretionary use MAPs. During the Dragon Boat Festival, it is common to hang wormwood and calamus on doors, as well as make and wear MAPs like sachets. These practices are the basis of our analysis of the correlation between MAPs and human health, as well as their significance in the Earth's ecosystem. It is hypothesized that MAPs play significant roles in Earth's ecosystems by interacting with organisms in their surroundings and affecting human health within the environment. To verify this hypothesis, the Aromatic Plant Environmental Health Engineering (APEHE) was designed, and relevant experiments were conducted.

2. Effects of plant secondary metabolites (SM) on organisms and differences in compounds between essential oils and living plant volatiles

For centuries, humans have used plant-produced organic compounds for pharmaceuticals or direct plants as herbal medicines for treating diseases, including antiviral activity against SARS-cov [6]. Approximately 25 % of drugs originate from plants [7,8], and biodiversity and drug acquisition also have a symbiotic relationship [9].

In plants, SM are classified into three categories: terpenes, phenolic compounds, and alkaloids, including volatile organic compounds (VOCs).

A variety of evidence shows that plants produce VOCs and external interaction [10], such as terpenes, which are the largest group in plant SM [11]. Terpenes have various biological functions, such as antibacterial, anti-worming, and resistance to pathogen attack [12, 13].

2.1. Effect of extracts containing volatile components of MAPs on microbiological

Plants have evolved multiple defense mechanisms to avoid viral, bacterial and fungal infections, and the antiviral mechanisms of plants stem from complex interactions between biochemical, genetic, and cellular factors [14].

Essential Oil (EO) (also known as volatile oil) is an aromatic oil liquid extracted from different parts of a plant (flowers, buds, seeds, leaves, branches, bark, herbs, wood, fruit and roots) [15]. The EO has been shown to possess antibacterial, antifungal, antiviral, antioxidant, and insecticidal properties. Furthermore, it has been demonstrated to be effective against drug-resistant microbes in reducing plaque [16–18]. Such as HSV-1 [19], HSV-2 [20–22], drug-resistant clinical herpes simplex virus type 1 strains [17], Bovine herpesvirus-1 [23], HIV-1 [24], SARS-COV [25].

In summary, plant extracts containing volatile components are primarily used to reduce and inactivate microbial growth through in vivo and in vitro administration routes:

- ①. In vitro interference with viral particles and/or viral envelope may mask the viral structures or cellular receptors required for viral adsorption and entry into host cells, attenuate viral activity, and act before viruses and bacteria bind to the human body.
- ②. In vivo, multistage interactions with viruses and the human body, such as competitive binding with viruses contact the host cell surface molecules and inhibit specific proteases to reduce or prevent virus adsorption, virus particles and host cell fusion process blocking the virus into the cell membrane, through the regulation of the immune system, such as anti-inflammatory, to indirect regulation of bacterial and viral infections in the human body [17,19–24,26–30].

Some experiments have shown that cinnamon bark, clove, thyme, peppermint, and citronella oils have the strongest activity in vapor and liquid systems for bacterial infections [31]. Tea tree and eucalyptus oil aerosol and vapor all have strong antiviral effects, capable of inactivating enveloped influenza A virus and nonenveloped *E. coli* phage M13, with an efficiency of over 95 % [32].

2.2. In vivo distribution investigations: differences between single components and blends of essential oils

When EO is absorbed and acts on the organism, the effect of the composition ratio of the organic compounds of EO may be different from the original ratio when EO is absorbed. For example, compared with a single compound component, the amount of α -pinene in the brain and liver after inhalation of mixed ingredients is twice that of single component inhalation. In the comparison of mixed inhalation components, the ratio of α -pinene increased to approximately three times that of 1,8-cineole [30].

2.3. Similarities and differences between essential oils and biological volatile organic compounds (BVOCs)

Variations in extraction methods, volatile organic compounds resulting from plant cell damage (e.g. friction and gnawing), and volatiles from normal plant growth can vary for numerous reasons. However, extracts of MAPs that are presented differently also have the same fraction of compounds. Take eucalyptol as an example:

The viral inhibitory capacity of seven major compounds in essential oils was revealed through molecular docking studies, and they were ranked according to their binding energy (ΔG), eucalyptol > alpha-pinene > alpha-terpineol > 3-carene > β -limonene > α -cymene > citronellol [33].

However, the same organic compounds, such as eucalyptol, in natural planting have the highest eucalyptol emission rates of $0.16 \pm 0.11 \text{ nmol m}^{-2} \text{ s}^{-1}$ observed for *Cinnamomum camphora* (*Lauraceae*) [34].

It follows that from a molecular chemical perspective, BVOCs and essential oils have the same major components, for example, both contain eucalyptol (1,8-cineole, known as eucalyptol). These intersections can be used to select the species of MAPs required for formulation within the environment. It is crucial to assess the interactions of these compounds in the natural environment, including the possibility of synergistic [35] antagonism.

3. Potential impacts of medicinal and aromatic plants (MAPs) on carbon fixation, nitrogen fixation, and global warming in artificially constructed green environments

The importance of carbon in global warming is widely known. Studies have shown that the restoration of forest land globally helps to capture atmospheric carbon and mitigate climate change [36], and anthropogenic disturbance can reduce carbon reserves in forest reserves [37].

Data suggest that the expansion of urban green space generally leads to environmental cooling and reduced CO₂ emissions [38], can integrate green infrastructure with high carbon storage and sequestration (CSS) into the urban mainstream [39], and can identify and cite carbon sequestration plant species that can be more quickly and efficiently [40].

Known patterns of intercropping of MAPs are superior to conventional planting. For example, *Piliostigma reticulatum* has been used for the traditional treatment of digestive diseases [41], and long-term intercropping with *P. reticulatum* significantly improved soil quality in terms of carbon and nutrients [42].

In addition, nitrogen is also an important element in the greenhouse effect. Although the relationship between microbes and the carbon and nitrogen cycle network is extremely complex [43], the higher nitrogen content may still help to warm the earth [44]. Intercropping aromatic plants caused a significant increase in soil organic and available N content, for example, from 2008 to 2010, basil intercropping soil available nitrogen content increased by 29.0 %, 11.8 % and 8.2 %, respectively [45]. While intercropping aromatic plants such as almond intercropped with *Thymus* sp. or legume and citrus, with a highly efficient irrigated intercropping system (HEIIS), increased soil microbial richness by 15 %, reduction in soil erosion by 94 %, and increased soil organic carbon by 50 % compared with single cropping [46]. Even common crops such as intercropping corn-potato can improve the humification and aromatization of soil dissolved organic carbon (DOC) at the same nitrogen level [47]. Other aromatic plants have higher yields at higher nitrogen contents [48]. Plant secondary metabolites and soil aromatization, as well as high carbon and nitrogen fixation, may promote each other within a certain range.

It is also beneficial to intercropping medicinal and aromatic plants, such as *Trigonella foenum-graecum* L. and *Cuminum cyminum* L., to help reduce the disease of *Cuminum cyminum* L. without the use of chemicals [49]. However, intercropping can also change the proportion and content of secondary metabolites in different plants [50].

The current intercropping mode, more than two or a few varieties of experiments, however, changes in co-dominance of plant species will significantly and adversely affect the proportion of soil organic carbon [51]. Therefore, when modelling and considering different scenarios, it is necessary to adapt the recipes for planted species while ensuring sufficient species diversity.

The emission of BVOCs can significantly affect regional ozone and aerosol chemistry [52]. The emission of biogenic volatile organic compounds (BVOCs) from vegetation, which is primarily composed of monoterpenes (C₁₀H₁₆), can result in the formation of secondary organic aerosols (SOA). This process can lead to climate cooling through the creation of forest aerosol cloud patterns [53]. The increase in global low clouds by only 4 % is sufficient to counteract the 2–3 °C global warming caused by the doubling of CO₂ [54].

Meanwhile, ozone with positive changes in isoprene emission at low light and high atmospheric gases, liquids and particles (GLPs) and negative changes at high light and low atmospheric GLPs, the responses of ozone to monoterpenes were negative [55]. The relationship between BVOCs and ozone is currently not well understood and requires further research.

4. Benefits of planting MAPs in other fields

- 4.1. Intercropping MAPs may also be an effective supplement to the integrated pest management (IPM) strategy [56].
- 4.2. The planting of MAPs can improve damaged and contaminated soil. Phytoremediation is economical, beautiful, and environmentally friendly and has great potential in stabilizing industrial waste [57].
- 4.3. In the field of circular economy, MAPs promote the circular economy and the in situ restoration of degraded and marginal land, providing various tangible and intangible benefits, including ecosystem services [58]. For example, outdoor MAPs intercropping and planting for some crops, such as betel nut, improves the resource utilization efficiency and the net rate of return per unit area [59].

At the same time, in addition to the beneficial effects of BVOCs of MAPs on the environment and the development of terpene fuel [60], compounds containing non-volatile components can also be extracted, such as the value of phenolic compounds [61] and carnosic acid (CA) [62]. After extracting the required compound components, plant fiber is also a recyclable material [63].

Simultaneously, since the ratio of C:N is higher for 5 years than for 10 or 15 years after planting [64], this provides a theoretical basis for planting MAPs in urban areas, collecting and recycling active ingredients for sustainable management, and replanting new MAPs for reproducible carbon and nitrogen fixation. Therefore, it is apparent that creating a functional environment to construct a green and recyclable industrial system, and generating economic benefits, is a practical and innovative direction for sustainable development.

- 4.4. We also need to distinguish between BVOCs and VOCs and examine their possible interactions. For example, studies have shown that growing common plants indoors can effectively remove 65–100 % of formaldehyde from polluted air [65].
- 4.5. It is worth noting that the atmospheric transformation of plant VOCs may alter their ecological roles. Relationships between volatiles and oxygenated substances and less volatile first-stage reaction products after oxidation with the atmosphere, such as verbenone, rosin aldehyde and *cis*-rosin acid, organic compounds that exist in an aerosol state and attach to the surface of objects within the environment and affect insects and plants through atmospheric chemical reactions [66]. From this perspective, the mixed configuration of MAPs within the environment may have an impact on the survival time of bacteria and viruses in aerosols and on the surface of objects.
- 4.6. In terms of carbon assets, increasing the carbon sink per mu of land can produce more carbon assets than in the existing way.

Taking monoculture forests as an example, which cover 264 million hectares worldwide [67]. The monoculture plantations sequestered 0.32 Mg ha⁻¹year⁻¹ of carbon. The harvesting rotation was set at 6 years, as sequestration in mixed forests peaks between 6 and 10 years [68]. In the available data, it was found that intercropping MAPs resulted in a 50 % increase in organic carbon [46].

Let r be the rate of soil carbon sequestration per hectare per year by monoculture forestry (0.32 Mg).

Let A be the area in square centimeters (264 million hectares).

6 years total fixed carbon margin (in Mg) = $r \times A \times 6 \times 0.5 = 253440000$ Mg.

It is possible to add an additional 0.25 Gt of carbon to the carbon sink every 6 years by considering the planting and harvesting cycle. This will create new value in the carbon asset space.

The examples provided only refer to monoculture plantations. However, it is also possible to reform areas of urban green space for mixed plantations. This excludes green roofs, vertical greening, and land with less than 2 m of mulch. Apart from urban green spaces, there are also barren hills and wastelands without vegetation that can be utilised.

The examples provided are approximate. Undoubtedly, the reality is more complex. Not all urban green spaces are monocultures, and carbon sequestration rates can vary between MAPs formulations. Factors such as climate, soil, plant species suitability, microbial communities, the continuous expansion of urban green spaces, and structural modifications of different urban buildings will all affect the value of carbon assets resulting from sequestration efficiency gains. This example only demonstrates the carbon asset potential of the MAPs planting model. Further experiments and more precise data are required to accurately quantify the calculation.

- 4.7. From the perspective of forest recuperation, the benefits of forest bathing for human mental and physical health are obvious [69,70], but in this process, it is necessary to pay attention to the difference between primeval forest and artificial forest. In view of the changes in modern people's living habits, human activities have become more intensive. While ensuring that humans do not excessively interfere with the remaining native natural forest ecological environment, creating a new, richer and more effective artificial forest restoration model in the city may be more suitable for the modern urban lifestyle.

Considering and discussing the above problems, we first constructed the following experimental model.

5. Theoretical method: theoretical design scheme of the APEHE system

This research direction of Aromatic Plants Environmental Health Engineering (APEHE) is a new cross-field systems engineering model in the environment through reasonable configuration of appropriate MAPs varieties and sufficient quantity, forming a "formula" through various methods such as regulating the environmental temperature and light to promote and more effectively use the interaction of volatile secondary metabolites such as terpenes in the environment, thus realizing the benefits of the environment for human mental and physical health.

Given the potential for transmission of disease-causing microorganisms both indoors and outdoors [71]. This system engineering model is divided into two parts: outdoor and indoor.

Outdoor: MAPs are formulated for use within city departments and enterprises responsible for managing and supervising green spaces. The primary objective is to increase carbon and nitrogen fixation of land, with sufficient biodiversity and suppression of microbial function and soothing serving as secondary objectives. To achieve this, design, empirical studies, and compositional measurements are employed to adjust ambient air quality and BVOC compositional content. Harvesting at carbon saturation is utilised for the production of plant extracts, animal feed [72], fermentation processes, etc., and recycling to cultivate new MAPs.

Indoors: The objective is to design an indoor space that can accommodate adequate amounts of MAPs formulations while controlling the appropriate light, temperature, and humidity. The primary goal is to combat disease-causing bacteria and viruses and transfer volatiles to connected indoor habitats. This can be achieved by connecting to a ventilated recirculation system, which exhausts the air from the habitats to the outside or recirculates it back to the plant growing space. The result is a holistic aromatic volatilizer gas recirculation system. The indoor space is open to the public for recreation and leisure, while regularly monitoring changes in the volatile composition of the indoor space, conducting sampling and analysis of pathogens, and making timely adjustments to MAPs formulations to ensure integrity. Additionally, appreciation of the landscape and to regulate the mood of the population [73].

Meanwhile, on the premise of meeting indoor needs, redundant BVOCs can be considered by some methods of enrichment and transformation and the recovery of MAPs [74], research and development of new fuels [75] or hybrid fuels [76] and applications in other fields, such as gas-powered nanosynthesizers for automatic production of polymers on demand [77].

We also need to manage the "damage", such as some plants being toxic to humans and animals [78]. The aim is to create a positive cycle of ecosystems that encourage biodiversity while preventing the unfair distribution and misuse of these MAPs. The experimental

Table 1
Plant variety, approximate size and quantity.

Plant variety, Approximate size, Quantity and Volatile reference				
Latin name	Size	Quantity	The main chemical types and compounds of MAPs	Proportion to total amount (gauge)
<i>Thuja orientalis</i> (<i>Platycladus orientalis</i> (L.) Franco)	2 m high	4	α -pinene; α -pinene/3-carene; cedrol; and cedrol/terpinyl acetate [79]	0.8
<i>Platycladus orientalis</i> (L.) Franco cv. <i>Aurea Nana</i>	0.8 m diameter	2		
<i>Juniperus procumbens</i> Sargent	1 m high	10	α -pinene; camphene; β -pinene; sabinene; myrcene; limonene; terpinolene;	
<i>Juniperus oxycedrus</i>	1.6 m high	3	linalool; camphor; β -caryophyllene; α -terpineol [80]	
<i>Juniperus chinensis</i> 'Globosa'	0.4 m diameter	6		
<i>Juniperus sabina</i> (<i>Sanina vulgaris</i> Antoine)	1 m high	5		
<i>Juniperus chinensis</i> Roxb.	2 m high	2		
<i>Cupressus arizonica</i> var. <i>glabra</i> 'Blue Ice'	2 gallons	1	α -pinene; umbellulone [81]	
<i>Cupressus macrocarpa</i> 'Gloderest'	0.4 m high	1	cupresins A–C; agathadiol; 19-hydroxy-13-oxo-15,16-dinor-entlabda-8 (17)-ene; isocupressic acid; acetyliscupressic acid; (–)-matairesinol; arctigenin; (–)-deoxydopodophyllotoxin [82]	
<i>Agastache foeniculum</i> (Pursh) Kuntze	2 m high	3	estragol; eugenol; methyl isoeugenol [83]	
<i>Agastache rugosa</i> (Fisch. et Mey.) O. Ktze.	1 m high	10	<i>p</i> -Menthan-3-one; estragole; pulegone [84]	
<i>Salvia leucantha</i> Cav.	2 gallons	4	bornyl acetate; β -caryophyllene; caryophyllene oxide; spathulenol [85]	
<i>Salvia farinacea</i> Benth.	1 gallons	2	1-octen-3-ol; (Z)-3-hexenal [86]	
<i>Artemisia indica</i> Willd.	0.5 m high	2	camphor; caryophyllene oxide [87]	
<i>Artemisia argyi</i> Lévl. et Van.	0.6 m high	10	α -Thujone; bornanone; terpinen-4-ol; <i>cis</i> -2-menthenol; borneol; <i>cis</i> -sabinol; α -terpineol; β -caryophyllene; caryophyllene oxide; neointermedeol [88]	
<i>Artemisia annua</i> L.	0.6 m high	10	Artemisia ketone; α -caryophyllene; germacrene D [88]	
<i>Rosmarinus officinalis</i> L.	2 gallons	2	1,8-cineole; α -pinene; camphor; bornyl acetate; borneol; camphene; α -terpineol; limonene; β -pinene; β -caryophyllene; myrcene [89]	
<i>Lavandula angustifolia</i> subsp. <i>angustifolia</i>	0.3 m high	2	Linalool; linalyl acetate; (E)- β -caryophyllene [90]	
<i>Origanum majorana</i> L.	0.6 m long	1	terpinen-4-ol; <i>cis</i> -sabinene hydrate; γ -terpinene; α -terpinene; α -terpineol; <i>p</i> -cymene; linalool [91]	
<i>Crossostephium chinense</i> Makino	0.15 m high	30	santolina triene; 1,8-cineole [92]	
<i>Chrysanthemum indicum</i> Linnaeus	0.3 m high	2	1,8-cineole; <i>o</i> -cymene; camphor; pinocarvone; chrysanthenyl acetate; bornyl acetate; <i>trans</i> -caryophyllene; terpinen-4-ol; umbellulone; <i>trans</i> -pinocarveol; <i>cis</i> -verbenol; borneol; α -terpineol; caryophyllene oxide; thymol [93]	
<i>Santolina chamaecyparissus</i> L.	2 gallons	8	Tetrapentacontane; eicosyl acetate; 2-methylhexacosane; <i>n</i> -pentadecanol [94]	
<i>Eucalyptus cinerea</i> F. Muell. ex Benth.	1.2 m high	4	1,8-Cineole; α -Terpineol; α -Pinene; Limonene; <i>p</i> -Cymene; <i>tr</i> -Pinocarveol; <i>tr</i> - <i>p</i> -Mentha-1,7, 8dien-2-ol [16]	
<i>Eucalyptus citriodora</i> Hook.f.	1.4 m high	2	Citronellol; Eucalyptol; 3-Carene; <i>D</i> -Limonene; α -Pinene; <i>o</i> -Cymene; α -terpineol [33]	
<i>Leptospermum scoparium</i>	0.7 m high	5	leptospermone; calamenene; δ -cadinene; cadina-1,4-diene; flavesone; cadina-3,5-diene; α -copaene; α -selinene; β -triketones; α -pinene [95]	
<i>Melaleuca alternifolia</i> (Maiden & Betche) Cheel	0.3 m high	4	terpinen-4-ol; γ -terpinene; 1,8-cineole [30]	
<i>Laurus nobilis</i>	0.6 m high	1	β -ocimene; 1,8-cineole; α -pinene; β -pinene [25]	
<i>Cinnamomum burmanni</i> (Nees & T. Nees) Blume	1.2 m high	3	3-carene; camphene; limonene [45]	
<i>Cinnamomum parthenoxylon</i> (Jack) Meisner	1.5 m high	2		
<i>Cinnamomim camphora</i> L.	1 m high	1		
<i>Cinnamomum japonicum</i> Sieb.	1.2 m high	1		
<i>Zanthoxylum schinifolium</i> Sieb. et Zucc.	0.7 m high	1	linalool; ar-tumerone; limonene; elixene [96]	
<i>Ajania pacifica</i> (Nakai) K. Bremer et Humphries	0.2 m high	5	camphor; (+/–)-lavandulol; eucalyptol [97]	
<i>Glechoma longituba</i> (Nakai) Kupr.	0.2 m long	10	dammarane; oleanane; ursane; lupinane; glecholone; 5 α -pinan-3-one-5-O- β -glucopyranoside; 2 α -pinan-3-one-2-O- β -glu-copyranoside; 11 α , 12 α -epoxy unit, glechomanosides A–E [98]	0.2
<i>Angelica polymorpha</i> Maxim.	0.2 m high	2	Imperatorin; isoimperatorin oxypeucedanin; psoralen; oxypeucedanin hydrate; byakangelicin; angeliticin; α -pinene; myrcene; <i>p</i> -cymene [99]	
<i>Vetiveria zizanioides</i> / <i>Chrysopogon zizanioides</i>	0.3 m high	2	α -Vetivones; β -Vetivones; γ -vetivenene; Sativene; Khusimene; β -Caryophyllene; α -Humulene; α -Amorphene; γ -Cadinene [100]	

(continued on next page)

Table 1 (continued)

Plant variety, Approximate size, Quantity and Volatile reference				
Latin name	Size	Quantity	The main chemical types and compounds of MAPs	Proportion to total amount (gauge)
<i>Lantana camara</i> L.	0.6 m diameter	2	Caryophyllene oxide; <i>n</i> -Hexadecanoic acid; Davanone; beta-Sesquiphellandrene [101]	
<i>Ruta graveolens</i> Linn.	0.5 m diameter	1	2-undecanone; 2-nonanone [102]	
<i>Pelargonium roseum</i> Willd.	1.6 m high	1	citronello; linalool; geraniol [103]	
<i>Michelia × alba</i> DC.	1.4 m high	1	linalool; α -terpineol; phenylethyl alcohol; β -pinene; geraniol [104]	
<i>Alpinia sichuanensis</i> Z.Y. Zhu	0.2 m high	4	b-sitosterol; kaempferol-3,4'-dimethylether; <i>p</i> -Hydroxybenzaldehyde; galangin; benzaldehyde; pinoembrin; 3-methoxybenzoic acid; isovanillic acid; <i>p</i> -coumaric acid; kaempferide-4'-methylether; (3R,4R,6S)-3,6-dihydroxy-1-menthene; sitosteryl- β -D-glucoside; dibutyl phthalate; kaempferol; kaempferol-3-O- β -D-glucopyranoside; hesperidin [105]	
<i>Mansoa alliacea</i> (Lam.) A.H. Gentry	0.9 m high	1	Chlorogenic acid; vanilic acid; caffeic acid; <i>p</i> -coumaric acid; ferulic acid; rutin; <i>trans</i> -cinnamic acid; luteolin; apigenin; betulinic acid [106]	
<i>Atractylodes lancea</i> (Thunb.) DC.	0.1 m high	1	elemol; β -selinene; atractylone [107]	
<i>Achyranthes aspera</i> L.	0.2 m high	10	N, N-Dimethylglycine; Phthalic acid, isobutyl 4-octyl ester; 1-Cyclohexylnonene; Hexadecanoic acid, methyl ester; 9,12-Octadecadienoic acid, methyl ester; 9,12,15-Octadecatrienoic acid, methyl ester, (ZZZ); Phytol; 9,12-Octadecadienoic acid; 4- <i>tert</i> -Butylcalyx [4] arene [108]	
<i>Levisticum officinale</i> Koch	0.15 m high	2	α -terpinenyl acetate; β - phellandrene; neocnidilide [109]	
<i>Solidago decurrens</i> Lour.	0.2 m high	1	α -pinene; β -pinene; myrcene; limonene; germacrene D; benzyl benzoate; β -caryophyllene [110]	
<i>Melia azedarach</i> L.	1 m high	1	β -caryophyllene; benzaldehyde; azulene [111]	
<i>Allium cepa</i> L.	0.1 m high	2	Acetone; dimethyl disulfide; hexanal [112]	
Varieties that grow in the soil with only a few leaves or only tender buds but may have allelopathic effects				
<i>Vitex rotundifolia</i> Linnaeus f.		4		
<i>Tetradium ruticarpum</i> (A. Jussieu) T. G. Hartley		5		
<i>Cinnamomum cassia</i> Presl		2		
<i>Asarum sieboldii</i> Miq.		10		

(*It should be noted that the compound references in Table 1 are primarily obtained from essential oils, plant tissue crushing, solvent extraction, and other methods of component detection. These compounds may differ from those volatilized in the air by plants during actual cultivation. The table should only be used as a reference when selecting the desired species based on their function. Subsequent experiments should aim to detect the actual volatiles. It may be necessary to make timely adjustments to the plant species and ratios.)

protocols within this paper are indoor.

6. Experimental materials and methods

6.1. Plant formula selection and environmental configuration

A comparison was made by searching the available literature for plant volatiles with antimicrobial activity. We selected plants of *Cupressaceae*, *Lamiaceae*, *Asteraceae*, *Myrtaceae*, *Lauraceae*, *Verbenaceae*, *Rutaceae*, etc. Specific plant species and quantities utilised are exhibited in Table 1.

In Hefei, Anhui Province, China, they were planted in a greenhouse measuring 4.8 m in length, 3 m in width, and 2.8–3.1 m in height, with an area of approximately 16 square metres. The room temperature is maintained between 5 and 35 °C throughout the year, and the relative humidity (RH) is approximately 45%–80 %.

6.2. Extraction methods and qualitative analysis of compounds in air, network pharmacology, and molecular docking

We tried three matching methods of organic solvents *n*-hexane (HEX) and HEX to dichloromethane (DCM) 1:1 and HEX to DCM to ethyl acetate 2:1:1.

We used an atmospheric constant current sampler and impact absorbent bottles in the collection, which was carried out at multiple points in the greenhouse. A brown glass bottle containing a mixture of organic solvents was passed through at a flow rate of 2 L of air per minute. The collection temperatures ranged from 20 °C to 35 °C, the relative humidity ranged from 45 % to 80 %, and the collection heights ranged from 60 cm to 150 cm. Close the greenhouse for at least 1 h prior to each collection. The average collection volume of approximately 70 ml of mixed organic solvent could enrich approximately 1 ml of liquid. After noticing residual compounds on the absorption bottle wall from the enriched liquid transfer tube, we washed it carefully with 2 ml of 95 % ethanol. We encapsulated the rinse solution in a separate test tube, which we later employed as the sample dissolution solution for gas chromatography-mass spectrometry (GCMS) analysis. GCMS analyses of solutions without 95 % ethanol fail because the aerosol is not uniformly

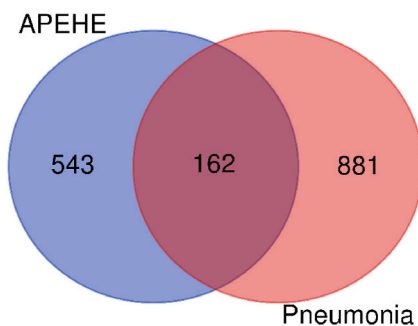


Fig. 1. Wayne diagram of potential APEHE and pneumonia targets.

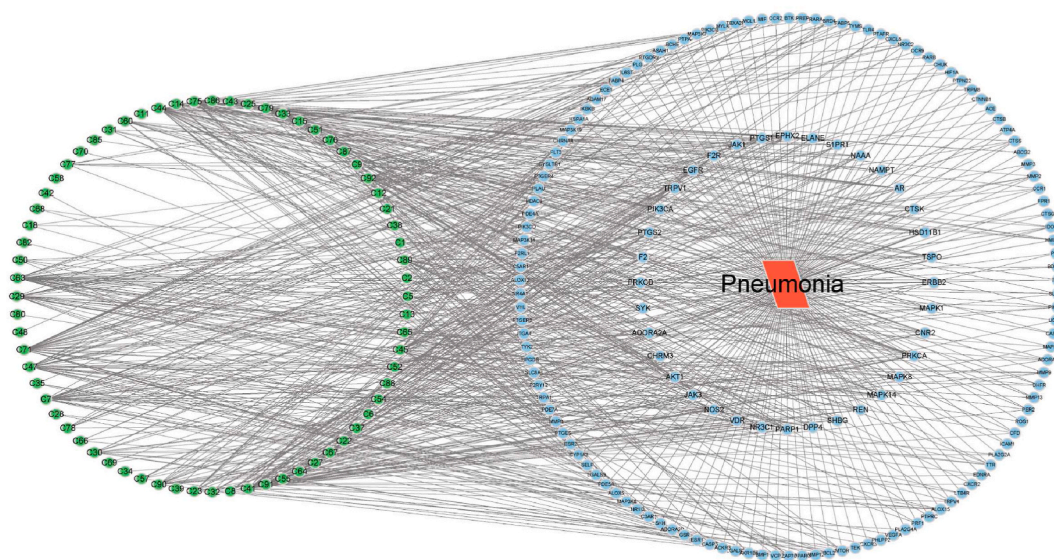


Fig. 2. APEHE active pharmaceutical ingredient - pneumonia disease target network (Note: Green nodes represent compounds and blue nodes represent pneumonia-related targets.). (For interpretation of the references to colour in this figure legend, the reader is referred to the Web version of this article.)

dispersed and is clearly stratified.

The GCMS analysis was conducted using an Agilent 7890B-5977A in SCAN mode. The electron ionisation system had an ionisation energy of 70 eV, a scan time of 2.5 s, and a mass range of 30–500 amu. The analysis was performed using an Agilent 19091S-433UI: HP-5MS Ultra Inert 0 °C–325 °C (350 °C): 30 m × 250 μm × 0.25 μm column with an initial flow rate of 1 mL/min, which was then increased to 1.5 mL/min. The GC autosampler was used in a non-split mode with an inlet port at 250 °C. The autosampler injected 1.0 μl of the sample, and the purge flow rate was set to 3 mL/min after 1 min. The column chamber temperature was initially set at 35 °C with a hold time of 0 min, and was run to 45 °C and then gradually increased at a rate of 5 °C/min, held at 60 °C for 5 min, and then increased at a rate of 15 °C/min to 280 °C, and held for a further 5 min. Confirmation and unambiguous identification were achieved by matching the mass spectrometry data of the detected compounds with the NIST17 MS library.

All samples were analysed by GCMS by Beijing QingXi Technology Research Institute. The reports are stored in publicly accessible databases, which can be accessed via the link provided in the Data Availability section.

The 2D sdf files of 93 compounds detected by GCMS were inputted into the SwissTargetPrediction platform. A total of 705 targets were screened with a probability threshold of ≥ 0.1 .

Three databases, MalaCards (<https://www.malacards.org/>), OMIM (<https://omim.org/>) and DisGeNET (<https://www.disgenet.org/>), were used to search for the disease target gene using “Pneumonia” as the search term, setting the species to human and obtaining the disease target genes. The disease targets retrieved from the databases were de-duplicated and merged, and 1043 disease targets were finally obtained.

The 705 targets of the screened drugs and the 1043 disease targets of pneumonia were intersected, imported into Venny 2.1 software and displayed as Wayne diagrams, and 162 intersected targets were obtained, which were used as potential targets of the drugs acting on the diseases for the subsequent analyses, as shown in Fig. 1.

A component target disease network diagram was then constructed using Cytoscape software, as shown in Fig. 2.

162 common targets were imported into DAVID Bioinformatics Resource 6.8 (<https://david.ncifcrf.gov/home.jsp>) for pathway and GO enrichment analyses, where GO analyses included biological process (BP), cellular component (CC) and molecular function (MF). Filtering was performed with a threshold of $P < 0.05$, and the top 10 enriched entries are shown in bar and bubble plots, respectively.

To construct the Protein-Protein Interaction (PPI) network, the drug-disease common targets were entered into the STRING database (<https://string-db.org/cgi/input.pl>), the biological species was set to 'Homo sapiens' and the threshold was set with the default parameters to obtain the PPI network. The TSV files obtained from the STRING database were imported into Cytoscape software and the topological analysis of the PPI network was performed using three centrality algorithms, including degree centrality, mediator centrality and proximity centrality algorithms. Thus, identifying the primary objective.

Molecular docking analysis was then performed. First, the crystal structures corresponding to the AKT1 protein (PDB ID: 7NH5 Chain A) and the TLR4 protein (PDB ID: 3FXI Chain A) were obtained from the RCSB PDB database, and for the EGFR, MMP9 and CXCL8 proteins without suitable crystals, their protein crystals were predicted using AlphaFold2. The Protein Preparation Wizard module of Schrödinger software was used for pre-processing, and the SiteMap and Receptor Grid Generation modules of Schrödinger were used to obtain the active sites of the proteins. Secondly, the 2D sdf structure files corresponding to the compounds were downloaded from the PubChem database and pre-processed using the LigPrep module in Schrödinger. Finally, all prepared ligand compounds were subjected to XP molecular docking and MM-GBSA analysis with the active sites of the five proteins.

6.3. Drug resistance rescue experiment

We found drug-resistant *Staphylococcus aureus* and drug-resistant *Bacillus cereus* in the nasal cavity of a 7-year-old child, drug-resistant *Bacillus subtilis* in the nasal cavity of a 66-year-old adult, and purchased drug-resistant *Pseudomonas aeruginosa*. All bacteria were sequenced for 16S rRNA by the Beijing QingXi Technology Research Institute (see Appendix BT230207005, BT23030515037).

The part of the collected liquid that was not dissolved in 95 % ethanol was used for the bacterial drug susceptibility experiment and the drug resistance rescue experiment. Due to limited conditions, we used naked eye turbidimetry, and the turbidity tube was provided by BKMAM. One microliter disposable inoculation ring and 0.9 ml LB broth could form a concentration of approximately M1. 100 μ l of various bacterial suspensions were evenly spread onto nutrient agar medium using a spreader. Once the bacterial solution was absorbed into the medium, the culture medium was inverted. To ascertain the bacterial strain's susceptibility, drug susceptibility paper was placed in several locations, including blank paper. Half of the discs were loaded with 40 μ l of APEHE liquid, extracted from air. Of these, only drug-resistant *Pseudomonas aeruginosa* was cultured for up to 3 h, and it died at a slightly higher concentration and/or a slightly longer time. The other three drug-resistant *Staphylococcus aureus*, drug-resistant *Bacillus cereus* and drug-resistant *Bacillus subtilis* strains were cocultured with liquid extracted from air for 24 h and then incubated on nutrient agar for 8–12 h to observe the effect of rescue drug resistance.

Simultaneously, the volatiles were found to contain several phthalates (PAEs). Dimethyl phthalate, Dibutyl phthalate, Dioctyl phthalate, and Diisooctyl phthalate were set at 10 %, while a bacterial co-culture was used as a control group.

6.4. Transcriptomics and metabolomics experiments in rescue drug-resistant *Staphylococcus aureus*

Correlation analyses were performed on metabolites and genes using transcriptomics and metabolomics. The study comprised three samples from each group: Experimental groups receiving extracts that showed a trend towards reduced resistance in plate cultures. Untreated control group of resistant bacteria. The experimental data were obtained from SHANGHAI BIOTREE BIOMEDICAL TECHNOLOGY CO. Details can be found in the data package.

In transcriptomics, the Truseqtm RNA Sample Prep Kit reagent was used to construct the library, but dUTP was used to replace dTTP in the dNTPs reagent used to synthesise the second strand of cDNA, so that the base in the second strand of cDNA contained a/U/C/g. Prior to PCR amplification, the second strand of cDNA was digested with ung enzyme so that only the first strand of cDNA was present in the library. Qubit2.0 was used for preliminary quantification and Agilent 2100 was used to determine the insert size of the library. The next experiment was performed when the insert size was as expected. After passing the library inspection, different libraries were pooled according to the target off-line data volume and sequenced on the second-generation high-throughput sequencing platform. Raw reads from the second-generation high-throughput sequencing platform were processed by removing low-quality sequences and connector contamination to obtain clean reads. All subsequent analyses were based on clean reads. Genomic sequences were compared, classified and characterised based on various genome annotations, and the corresponding expression levels were determined. Subsequently, differential expression analysis was conducted including GO enrichment and KEGG analysis.

We identified 187 genes that were differentially expressed, with 102 demonstrating up-regulation and 85 showing down-regulation. These genes were then mapped onto the KEGG database, which yielded 34 pathways.

In the metabolomics, add 250 μ L of water to the sample, then grind it for 4 min at 35 Hz and use ultrasound for 5 min in an ice water bath. Use 50 μ L of homogenate to determine the protein content. For extraction, take 200 μ L of homogenate and add 800 μ L of pre-cooled extract (−40 °C) consisting of methanol and acetonitrile in a 1:1 ratio. Stir for 30 s by vortexing (without the isotope-labelled internal standard mixture). Carry out ultrasonic treatment for 10 min in an ice water bath. Place the mixture in a −40 °C environment for 1 h. Afterwards, evaporate 800 μ L of the supernatant and then add the extract, which is composed of a combination of methanol, acetonitrile, and water in a 2:2:1 ratio with an isotope-labelled internal standard mixture, based on quantitative results of the protein. The sample is then centrifuged at 4 °C and 12,000 rpm for 15 min. Finally, transfer the supernatant to an injection vial. The liquid sample was supplemented with an equal volume of Quality Control (QC) to enable machine detection. The target compound was separated using a liquid chromatography column packed with a water-based Acquity UPLC BEH Amide (2.1 mm \times 50 mm, 1.7 μ m). For

Table 2
Compound C1–C93.

NO	Compound name	Cas	Compound CID
C1	1-Pentene,4,4-dimethyl-1,3-diphenyl-1-(trimethylsilyloxy)-		5378121
C2	4-hexene-2-one	25659-22-7	5326164
C3	2-ethyl-1-hexanol	104-76-7	7720
C4	Cyclopentasiloxane,decamethyl-	541-02-6	10913
C5	Cyclohexasiloxane,dodecamethyl-	540-97-6	10911
C6	Acetaminophen	103-90-2	1983
C7	Ethyl iso-allocholate	47676-48-2	6452096
C8	9-Octadecen-12-ynoic acid, methyl ester	56847-05-3	5363161
C9	Cyclododecanone, thiosemicarbazone		690106
C10	1-Butanol,3-methyl-		31260
C11	Muramic acid		441038
C12	2-Pentanol,3-methyl	565-60-6	11261
C13	Phenol	108-95-2	996
C14	1-Hexanol,2-ethyl-	104-76-7	7720
C15	Hexanoic acid,2-ethyl	149-57-5	8697
C16	Ethanol,2-(2-butoxyethoxy)-	112-34-5	8177
C17	Dodecane	112-40-3	8182
C18	3-Butyl-4,5-dimethyl-4-hydroxyhexahydropyrimidin-2-thione	88070-31-9	5363350
C19	Octasiloxane,1,1,3,3,5,5,7,7,9,9,11,11,13,13,15,15-hexadecamethyl	19095-24-0	6329087
C20	Acetic acid	64-19-7	176
C21	Silanediol,dimethyl-	1066-42-8	14014
C22	Hexadecane	544-76-3	11006
C23	Caprolactam	105-60-2	7768
C24	Heptaethylene glycol monododecyl ether	3055-97-8	76459
C25	Triphenylphosphine oxide	791-28-6	13097
C26	1-Butanol,3-methoxy-	2517-43-3	17291
C27	Dimethyl phthalate	131-11-3	8554
C28	9-Octadecenoic acid, (2-phenyl-1,3-dioxolan-4-yl)methylester, <i>cis</i> -		21160048
C29	<i>n</i> -Hexadecanoic acid		985
C30	Dibutyl phthalate	84-74-2	3026
C31	3,4'-Isopropylidenediphenol	46765-25-7	688289
C32	7-Isopropyl-4-morpholinomethyl-2-azulenamine		608036
C33	Flurbiprofen	5104-49-4	3394
C34	Octadecane,3-ethyl-5-(2-ethylbutyl)-	55282-12-7	292285
C35	Hexadecanoic acid, (2-phenyl-1,3-dioxolan-4-yl)methylester, <i>cis</i> -	18418-22-9	536555
C36	Bis(2-ethylhexyl)phthalate	117-81-7	8343
C37	Benzenedicarboxylic acid, bis(2-propylpentyl) ester	70910-37-1	191964
C38	Cyclotrisiloxane,hexamethyl-	541-05-9	10914
C39	3-Hydroxy-4-methoxybenzaldehyde,TBDMS	621-59-0	12127
C40	Azetidene,3-methyl-3-phenyl-	5961-33-1	22249
C41	Cyclotetrasiloxane,octamethyl-	556-67-2	11169
C42	2,5-Dihydroxybenzaldehyde,2TMS derivative	56114-69-3	622536
C43	Benzene,1-fluoro-4-(2-phenylethenyl)-,(E)-	718-25-2	5375540
C44	Ethanone,1-(2'-fluoro [1,1'-biphenyl]-4-yl)-	345-55-1	67662
C45	Flurbiprofen methyl ester	66202-86-6	4127
C46	Hydrogen bromide	10035-10-6	260
C47	4-methyl-2,4-bis(<i>p</i> -hydroxyphenyl)penta-1-ene,2TMS derivative	13464-24-9	83494
C48	2,4-Di- <i>tert</i> -butylphenol	96-76-4	7311
C49	Cyclooctasiloxane,hexadecamethyl-	556-68-3	11170
C50	Cyclononasiloxane,octadecamethyl-	556-71-8	11172
C51	1,2-Benzenedicarboxylic acid,bis (2-methylpropyl)ester	84-69-5	6782
C52	Tetrapentacontane,1,54-dibromo		545963
C53	7,9-Di- <i>tert</i> -butyl-1-oxaspiro (4,5)deca-6,9-diene-2,8-dione	82304-66-3	545303

(continued on next page)

Table 2 (continued)

NO	Compound name	Cas	Compound CID
C54	l-(+)-Ascorbic acid 2,6-dihexadecanoate	4218-81-9	54722209
C55	7,8-Epoxyolanostan-11-ol,3-acetoxy		541562
C56	Octasiloxane,1,1,3,3,5,5,7,7,9,9,11,11,13,13,15,15-hexadecamethyl-	19095-24-0	6329087
C57	2,4,6-Cycloheptatrien-1-one,3,5-bis-trimethylsilyl-		610038
C58	o-Vanillin,TBDMS	148-53-8	8991
C59	Octadecane,1,1'-[1,3- propanediylbis (oxy)] bis -	17367-38-3	624534
C60	Phenol,2,2'-methylenebis [6-(1,1-dimethylethyl)-4-methyl	119-47-1	8398
C61	1,4-Benzenedicarboxylic acid,bis (2-ethylhexyl)ester	6422-86-2	22932
C62	Heptasiloxane,1,1,3,3,5,5,7,7,9,9,11,11,13,13-tetradecamethyl	19095-23-9	6329088
C63	Butanoic acid,4-chloro-,1,1a,1b,4,4a,5,7a,7b,8,9-decahydro-4a,7b-dihydroxy-3-(hydroxymethyl)-1,1,6,8-tetramethyl-5-oxo-9aH-cyclopropa [3,4]benz [1,2-e]azulene-9,9a-diylester, [1aR-(1a.alpha.,1b.beta.,4a.beta.,7a.alpha.,7b.alpha.,8.alpha.,9.beta.,9a.alpha	37558-16-0	37783
C64	Androst-4-en-3-one,17-methoxy-,3-methoxime, (17.beta.)-		91712453
C65	Octadecane,3-ethyl-5-(2-ethylbutyl)-	55282-12-7	292285
C66	Octadecanal,2-bromo-	56599-95-2	537255
C67	7,13-Docosadienoic acid, pyrrolidide		91705104
C68	Hexadecane,2,6,10,14-tetramethyl	638-36-8	12523
C69	Hexadecanoic acid,1-(hydroxymethyl)-1,2-ethanediyl ester	40290-32-2	99931
C70	4a,7a-Epoxy-5H-cyclopenta [a]cyclopropa [f]cycloundecen-4(1H)-One,2,7,10,11-tetrakis (acetyloxy)decahydro-8,9-dihydroxy-1,1,3,6,9-pentamethyl-	51906-05-9	538560
C71	2-Butenedioic acid,1,4-bis(2-ethylhexyl) ester	128111-61-5	57347398
C72	Benzamide,2,4-dichloro-N-(2,2,2-trichloro-1-phenylsulfonyl)ethyl-		599621
C73	4H-Cyclopropa [5',6']benz [1',2':7,8]azuleno [5,6-b]oxiren-4-one,8,8a-bis(acetyloxy)-2a-[(acetyloxy)methyl]-1,1a,1b,1c,2a,3,3a,6a,6b,7,8,8a-dodecahydro-3,3a,6b-trihydroxy-1,1,5,7-tetramethyl-	77646-26-5	538186
C74	Chloriodomethane	593-71-5	11644
C75	Tetracosane	646-31-1	12592
C76	1,2-Benzenedicarboxylic acid, butyl octyl ester	84-78-6	66540
C77	2-Propenoic acid,3-(4-methoxyphenyl)-,2-ethylhexyl ester		5355130
C78	Octadecanoic acid, ethyl ester	111-61-5	8122
C79	1H-Cyclopropa [3,4]benz [1,2-e]azuleno-5,7b,9,9a-tetrol,1a,1b,4,4a,5,7a,8,9-octahydro-3-(hydroxymethyl)-1,1,6,8-tetramethyl-,5,9,9a-triacetate, [1aR-(1a.alpha.,1b.beta.,4a.beta.,5.beta.,7a.alpha.,7b.alpha.,8.alpha.,9.beta.,9a.alpha.)]-	77508-64-6	101280823
C80	Ethyl Acetate	141-78-6	8857
C81	4H-Cyclopropa [5',6']benz [1',2':7,8]azuleno [5,6-b]oxiren-4-one, 8-(acetyloxy)-1,1a,1b,1c,2a,3,3a,6a,6b,7,8,8a-dodecahydro-3a,6b,8a-trihydroxy-2a-(hydroxymethyl)-1,1,5,7-tetramethyl-, [1aR-(1a.alpha.,1b.beta.,1c.alpha.,2a.alpha.,3a.beta.,6a.alpha.,6b.alpha.,7.alpha.,8.beta.,8a.alpha.)]-	77573-35-4	101288159
C82	Silanediol, dimethyl	1066-42-8	14014
C83	3,5-Dihydroxybenzamide	3147-62-4	76604
C84	Cyclotrisiloxane,hexamethyl-	541-05-9	10914
C85	Oxime-,methoxy-phenyl-	67160-14-9	9602988
C86	Cyclohexene-,3,3,5,5-tetramethyl-1-(trimethylsilyloxy)-	143586-27-0	611062
C87	Cycloheptasiloxane,tetradecamethyl-	107-50-6	7874
C88	9-Octadecenoic acid, (2-phenyl-1,3-dioxolan-4-yl)methyl ester,cis		21160048
C89	Methanesulfonic acid, TBDMS derivative		14414886
C90	2-[(Trimethylsilyloxy)-2-{4-[(trimethylsilyloxy)phenyl]ethanamine		14345507
C91	1b,4a-Epoxy-2H-cyclopenta [3,4]cyclopropa [8,9]cycloundec [1,2-b]oxiren-5 (1aH)-one,2,7,9,10-tetrakis (acetyloxy) decahydro-3,6,8,8,10a-pentamethyl	51906-06-0	536452
C92	Propanoic acid,2-methyl-,3-hydroxy-,2,4-trimethylpentyl ester	77-68-9	6490
C93	Propanoic acid,2-hydroxy-,ethyl ester,(L)-	687-47-8	92831

this task, Thermo Fisher Scientific's Vanquish ultra-performance liquid chromatograph was employed. In liquid chromatography Phase A, an aqueous solution was employed, which contains 25 mmol/L ammonium acetate and 25 mmol/L ammonia water. Phase B comprises primarily acetonitrile. The injection volume was 2 μ L and the sample tray was kept at 4 $^{\circ}$ C. To process the data, the original data was converted to mzXML format using ProteoWizard software. The peaks were then detected, extracted, aligned and integrated using the R software package, which integrated XCMS. Afterwards, the data was compared with the self-constructed database biotredb (v2.1) using secondary mass spectrometry. An algorithm score cutoff value of 0.3 was used for the analysis.

After data preprocessing, hierarchical cluster analysis (HCA), metabolite classification statistics, univariate statistical analysis including student's t-test, Principal component analysis (PCA), Orthogonal Projections to Latent Structures- Discriminant Analysis (OPLS-DA), and others. Differential screening and identification of compounds, hierarchical cluster analysis of different metabolites,

Table 3

A portion of interesting compounds.

Compounds	Beneficial features	Risk	Interact
Flurbiprofen	Reducing protein aggregation and alleviating leptin resistance induced by stress, inhibiting the interaction between HH1R and PTEN displays anti-tumour effects on thyroid cancer, COX inhibitor, protects the hippocampal neurons [117–119], Acts directly in the central nervous system (CNS) through nose-to-brain delivery and surpasses intravenous administration [120].		Antagonistic
dibutyl phthalate (DBP)		Glucolipid metabolism [121], neurological effects [122], carcinogenicity, and immunotoxicity [123].	
Acetaminophen	Analgesia by inhibition of prostaglandin synthesis in the central nervous system [124].	Oral overdose can damage the liver, use during pregnancy may be unsafe, asthma, allergies, enhances the effects of warfarin and increases the risk of haematological malignancies [124].	
2,4-Di- <i>tert</i> -butylphenol	Antioxidant and anti-inflammatory, protects nerve cells from reactive oxygen species [125]. antibacterial [126]. anticancer [127]. antidiabetic effects [128].	Impairs bone cell differentiation [129], degradable by ozone [130].	
3-Hydroxy-4-methoxybenzaldehyde	Antioxidant, antibacterial, antifungal, antidiabetic, anti-inflammatory, analgesic and anticancer activities [131].		
1-(+)-Ascorbic acid 2,6-dihexadecanoate	Antioxidant [132]		
2-ethyl-1-hexanol		Respiratory toxicity endpoints of the TTC (Threshold of Toxicological Concern) for routine inhalation are set at 1.4 mg/day [133].	
Caprolactam	Cytotoxic against human epidermoid carcinoma (KB) cells and human colorectal adenocarcinoma (LoVo) cells and to have antiviral activity against herpes simplex II virus [134], and the related compound N-vinylcaprolactam has been shown to have anti-HIV activity [135].		
Oxime-,methoxy-phenyl-Triphenylphosphine Oxide	Inhibitors of influenza H1N1 [136]. Ir(III)-catalyzed C H functionalization of Triphenylphosphine Oxide toward 3-aryl-oxindoles [137].		
3-Methyl-1-butanol	Fuel substitute [138].		

box plot analysis, matchstick diagram analysis of different metabolites, radar diagram analysis of different metabolites, correlation analysis of different metabolites, chord analysis of different metabolites, KEGG annotation of different metabolites, KEGG enrichment analysis of different metabolites, pathway analysis of different metabolites, and network analysis of different metabolites.

We have identified a total of 6725 metabolites with detectable differences. Out of these, 3146 metabolites were up-regulated, whereas 3579 were down-regulated. The mapping of these metabolites on the KEGG database unveiled their distribution throughout 55 pathways.

Subsequently, a joint analysis was conducted on the two omics.

We performed hierarchical clustering analysis on the significantly different genes and metabolites using a correlation coefficient of $r > 0.8$ or $r < -0.8$ matrix heatmap. A complete chaining approach was used to cluster the differentially expressed metabolites and genes based on the Euclidean distance matrix (EDM).

6.5. Data availability

All relevant information has been deposited in the OSF repository under the registered DOI: <https://doi.org/10.17605/OSF.IO/9HF5P>.

7. Experimental results

7.1. GCMS results

The 93 compounds detected by GCMS were found in PubChem (<https://pubchem.ncbi.nlm.nih.gov/>) and named in the form of C1–C93 numbers. Specific information is given in Table 2.

In the GCMS detection report, surprising aspects is the different interesting medicinal constituents and intermediates and compounds that can be found at different times of the year, depending on the formula, number and growth of MAPs. This has not been previously discovered and may be linked to reduced indoor air flow, temperature and humidity fluctuations, various chemical reactions and photocatalysis [113], along with the theory that low carbon olefins cannot be emitted in space in time to react with each other and produce more stable large compounds [114]. Table 3 provides details on specific compounds, functions, and risks. It is

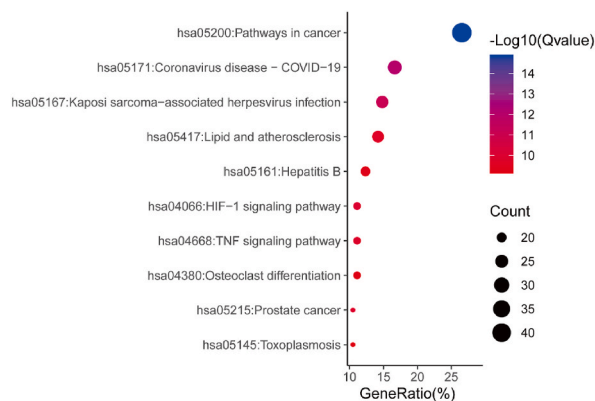


Fig. 3. Top 10 significantly enriched KEGG pathways.

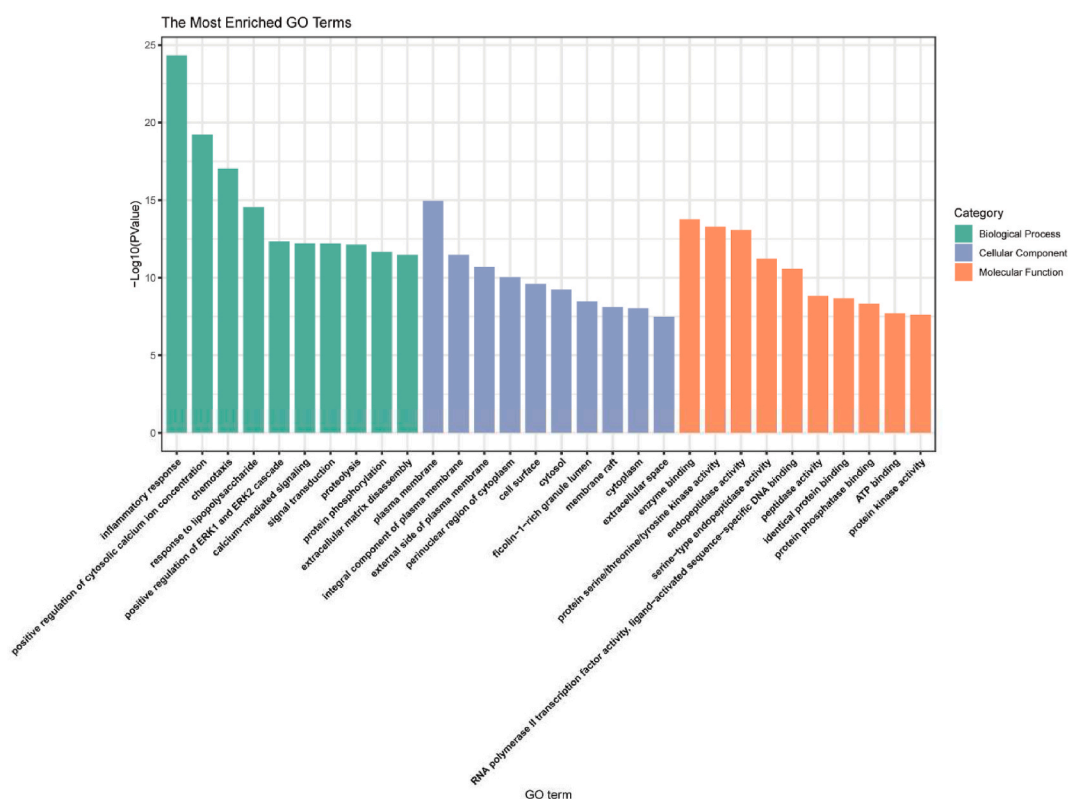


Fig. 4. GO enrichment analysis.

important to note that our experimental method involves enrichment and dissolution using an organic solvent and atmospheric sampler to assist in GCMS detection, which is limited by the experimental conditions. The alcohols in the solvent, such as ethanol, can allow many organic compounds to decompose or be synthesized, such as phthalic anhydride and the corresponding alcohol to form phthalic acid esters (PAEs) [115], and the appearance of more toxic and persistent intermediates in the photodegradation of dimethyl phthalate (DMP) in dichloromethane (DCM), whereas dioctyl phthalate (DOP) during photochemical transformation in organic solvents reduces the health risk to the human body [116]. As the sample age, the compounds they contain change and decrease over time. This sampling process may lead to disparities between the GCMS results and the original components of the surrounding atmosphere. Consequently, it is essential to employ alternative experimental methods and more appropriate testing equipment to determine the specific organic compounds present in the environment during MAPs growth.

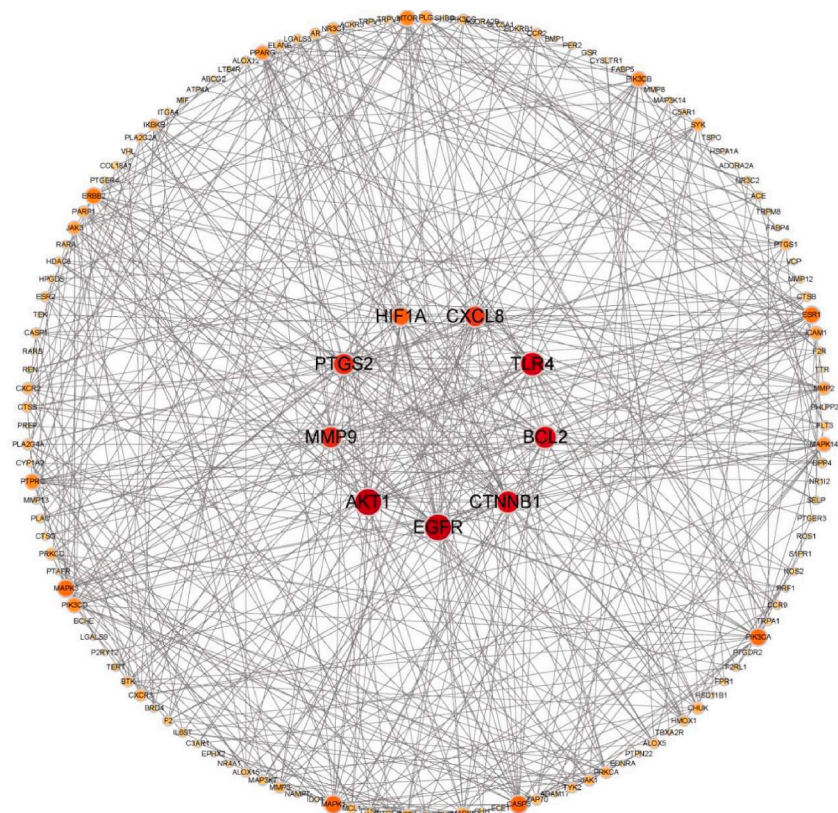


Fig. 5. Protein-protein interaction network.

Table 4

Top 10 results for PPI network topology analysis based on three centrality algorithms.

Target name	Degree centrality	Target name	Betweenness centrality	Target name	Closeness centrality
EGFR	37	PTGS2	0.17	EGFR	0.50
AKT1	37	CXCL8	0.15	MMP9	0.49
TLR4	32	EGFR	0.12	TLR4	0.49
BCL2	30	TLR4	0.12	AKT1	0.48
CTNNB1	30	MMP9	0.12	CTNNB1	0.48
MMP9	28	AKT1	0.10	CXCL8	0.47
PTGS2	28	PLG	0.07	PTGS2	0.47
CXCL8	27	F2	0.06	BCL2	0.45
HIF1A	23	PTPRC	0.06	CASP3	0.44
MAPK1	22	BCL2	0.06	HIF1A	0.44

(*The data package includes file APEHE_Network_Pharmacology (05122023) with complete data).

7.2. Network pharmacology and molecular docking results

The pathway enrichment analysis revealed the three pathways with the highest enrichment among the 162 shared targets: ‘hsa05200:Pathway in cancer’, ‘hsa05171:Coronavirus disease-COVID-19’, ‘hsa05167:Kaposi sarcoma-associated herpesvirus infection’ (Fig. 3).

GO enrichment analyses showed that the main biological process enriched was ‘inflammatory response’, the main cellular component enriched was ‘plasma membrane’ and the main molecular function enriched was ‘enzyme binding’ (Fig. 4).

Fig. 5 shows the protein-protein interaction network and highlights five main objectives. These objectives are represented by larger nodes and different colours.

Table 4 presents the top ten ranked data from the three centrality algorithms. The overall ranking includes EGFR, AKT1, TLR4, MMP9, and CXCL8 as the top five targets. These targets were selected as key targets for the PPI network and have been highlighted in the table for clarity.

Among these five proteins, AKT1 docking had 24 compounds, MMP9 and TLR4 had one compounds each, XP Gscore was less than

Table 5
Molecular docking results.

Compound	Cas	Compound CID	XP GScore	MM-GBSA dG Bind(kcal/mol)
Target AKT1				
Flurbiprofen methyl ester	66202-86-6	4127	-8.053	-44.67
7-Isopropyl-4-morpholinomethyl-2-azulenamine		608036	-7.813	-31.73
4-methyl-2,4-bis(<i>p</i> -hydroxyphenyl)penta-1-ene,2TMS derivative	13464-24-9	83494	-7.603	-38.71
3,4'-Isopropylidenediphenol	46765-25-7	688289	-7.477	-36.15
Hexadecanoic acid, (2-phenyl-1,3-dioxolan-4-yl)methylester, <i>cis</i> -	18418-22-9	536555	-7.338	-35.44
1,2-Benzenedicarboxylic acid, butyl octyl ester	84-78-6	66540	-7.167	-39.23
2,4-Di- <i>tert</i> -butylphenol	96-76-4	7311	-7.158	-30.04
Ethanone,1-(2'-fluoro [1,1'-biphenyl]-4-yl)-	345-55-1	67662	-7.126	-45.91
Phenol,2,2'-methylenebis [6-(1,1-dimethylethyl)-4-methyl	119-47-1	8398	-6.952	-46.03
9-Octadecenoic acid, (2-phenyl-1,3-dioxolan-4-yl)methylester, <i>cis</i> -		21160048	-6.793	-46.38
Dimethyl phthalate	131-11-3	8554	-6.622	-35.55
1,4-Benzenedicarboxylic acid,bis (2-ethylhexyl)ester	6422-86-2	22932	-6.349	-52.02
Triphenylphosphine oxide				
7,9-Di- <i>tert</i> -butyl-1-oxaspiro (4,5)deca-6,9-diene-2,8-dione	791-28-6	13097	-6.185	-37.61
	82304-66-3	545303	-6.137	-31.65
2,5-Dihydroxybenzaldehyde,2TMS derivative				
Bis(2-ethylhexyl)phthalate	117-81-7	8343	-6.041	-31.03
3-Hydroxy-4-methoxybenzaldehyde,TBDMS	621-59-0	12127	-6.046	-36.29
7,13-Docosadienoic acid, pyrrolidide		91705104	-5.994	-46.92
Benzene,1-fluoro-4-(2-phenylethenyl)-,(E)-	718-25-2	5375540	-5.98	-41.48
Heptaethylene glycol monododecyl ether	3055-97-8	76459	-5.565	-48.34
<i>o</i>-Vanilin,TBDMS				
Benzamide,2,4-dichloro-N-(2,2,2,-trichloro-1-phenylsulfonylethyl)-		599621	-5.498	-41.17
Dibutyl phthalate	84-74-2	3026	-5.279	-43.91
Oxime-,methoxy-phenyl-	67160-14-9	9602988	-5.16	-31.87
Target EGFR				
Muramic acid		441038	-6.835	-8.41
Butanoic acid,4-chloro-,1,1a,1b,4,4a,5,7a,7b,8,9-decahydro-4a,7b-dihydroxy-3-(hydroxymethyl)-1,1,6,8-tetramethyl-5-oxo-9aH-cyclopropa [3,4]benz [1,2- <i>e</i>]azulene-9,9a-diylester, [1a-(1a.alpha.,1b.beta.,4a.beta.,7a.alpha.,7b.alpha.,8.alpha.,9.beta.,9a.alpha	37558-16-0	37783	-4.788	-30.15
Target MMP9				
Muramic acid		441038	-7.915	-28.35
3,5-Dihydroxybenzamide	3147-62-4	76604	-5.571	-34.31
Target TLR4				
Muramic acid		441038	-6.637	-19.62
4H-Cyclopropa [5',6']benz [1',2':7,8]azuleno [5,6- <i>b</i>]oxiren-4-one, 8-(acetyloxy)-1,1a,1b,1c,2a,3,3a,6a,6b,7,8,8a-dodecahydro-3a,6b,8a-trihydroxy-2a-(hydroxymethyl)-1,1,5,7-tetramethyl-, [1a-(1a.alpha.,1b.beta.,1c.alpha.,2a.alpha.,3a.beta.,6a.alpha.,6b.alpha.,7.alpha.,8.beta.,8a.alpha.)]-		101288159	-5.029	-37.8
Target CXCL8				
Muramic acid		441038	-5.636	-23.65

-5 and MM-GBSA dG Bind was less than -30 kcal/mol, indicating that the free energy of binding was low and the ligand was stable in binding to the protein. Details are given in Table 5.

The specific docking situation of the molecule with the most stable binding of each protein is shown in Figs. 6-10:

The APEHE primary model's atmospheric compounds primarily bind to AKT1, with MMP9 and TLR4 acting as secondary binding agents, indicating a link to pneumonia. AKT1 is widely distributed throughout various human tissues, plays a crucial role in both broad-spectrum antiviral therapy include COVID-19 [139], chronic obstructive pulmonary disease (COPD) [140] and Cancer field [141].

7.3. Results of rescue drug resistance experiments

In the rescue drug-resistant experiment, we found that the resistant bacteria after coculture and enrichment solution reversed drug resistance to varying degrees. See Table 6 and images in Appendix 1.

After repeated experiments, drug-resistant *Staphylococcus aureus* showed the most significant and stable effect at 1:4. After culturing with a 1:4 extraction solution, we repeatedly subcultured the bacteria from the previous plate culture to the M1

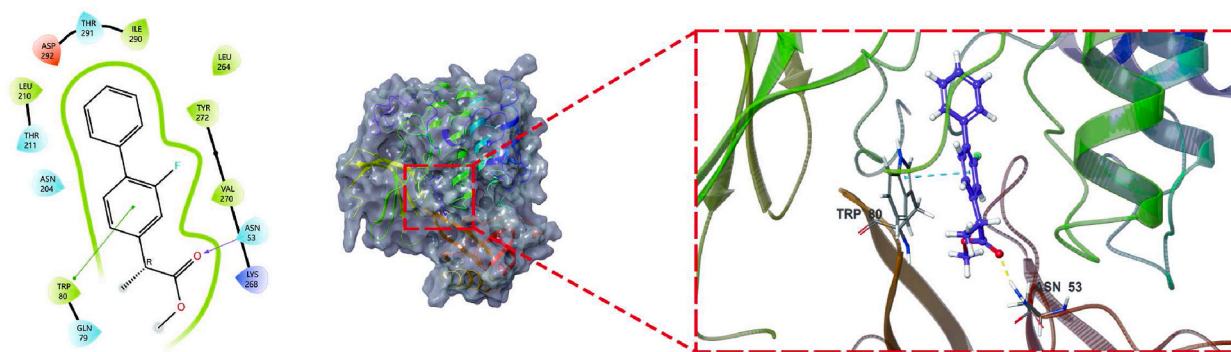


Fig. 6. The binding of flurbiprofen methyl ester to the AKT1 protein in both 2D and 3D formats.

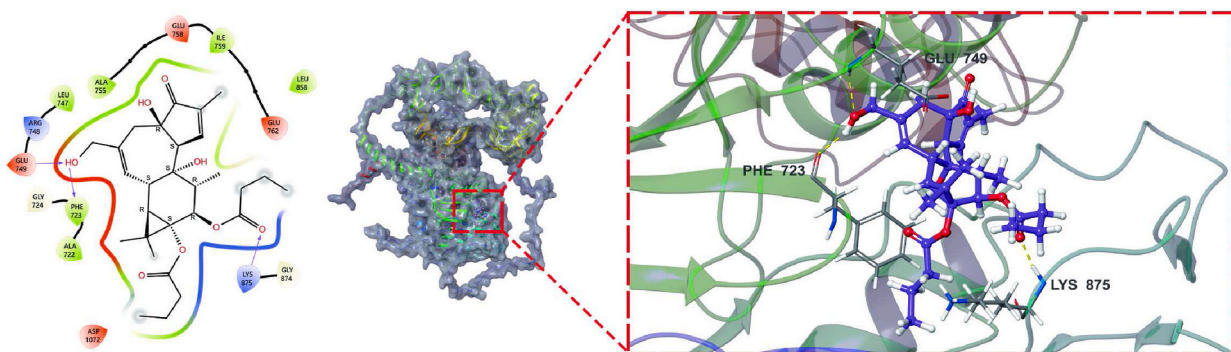


Fig. 7. The binding of 37,783 to the EGFR protein in both 2D and 3D formats.

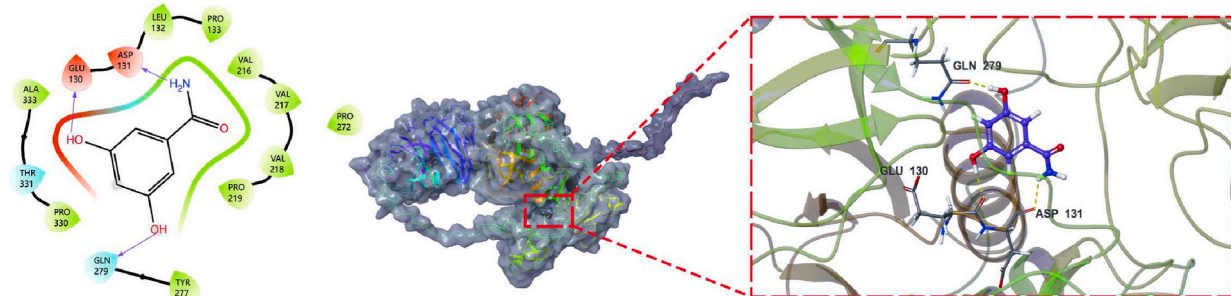


Fig. 8. The binding of 76,604 to the MMP9 protein in both 2D and 3D formats.

concentration. After changing from 1:4 to 1:1, then to 1:1 and then to 1:2, we still retained some degree of rescue drug resistance without coculturing with the extraction solution. Rescue drug resistance in drug-resistant *Pseudomonas aeruginosa* was not as effective as direct death, and penicillin was not effective. Drug-resistant *Bacillus cereus* and drug-resistant *Bacillus subtilis* effective penicillin at a 1:20 high dose, but seven consecutive days of low doses were not as effective as high-dose 24-h cocultures. The antibacterial zone where the extraction solution is replenished during cultivation of all nutrient agar media is always more pronounced than the zone where it is not replenished after cocultivation.

A 10 % control group of PAEs also exhibited some rescue drug-resistant effect. The extract was more effective than the PAEs alone, as evidenced by the difference in the size of the bacteriostatic circle.

We do not know whether the existence of PAEs is because the greenhouse material for the visor, plastic pot, the plant itself is volatile, the experimental process of mask and glove contamination [142], or multiple factors, but in the same period, we compared the PAEs collected outdoors and indoors and found no difference for PAEs (see Appendix BT220819030).

DMP is known to affect the activity of several bacteria [143–146], and many plants, such as *Osmanthus fragrans*, Black tea, Crabapple (*Malus sp.*) fruit, and the same composition has been found in volatiles [147–150]. Microbial *Pseudomonas* also uses three

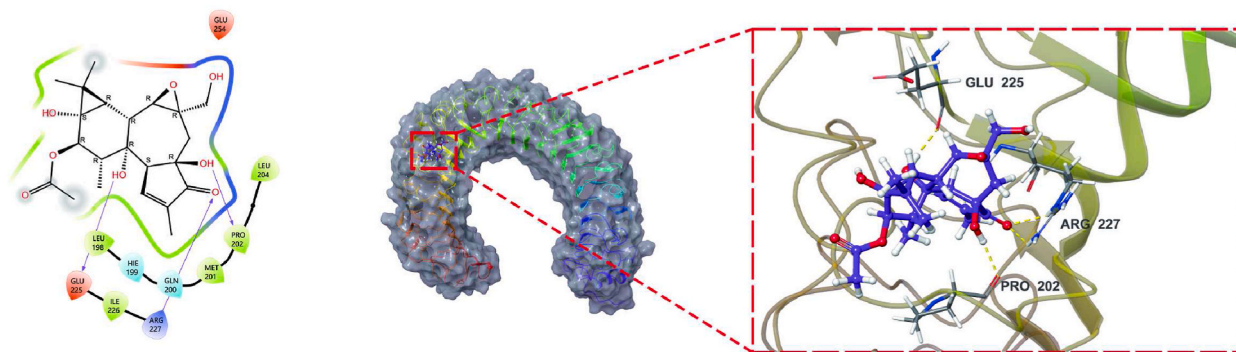


Fig. 9. The binding of 101288159 to the TLR4 protein in both 2D and 3D formats.

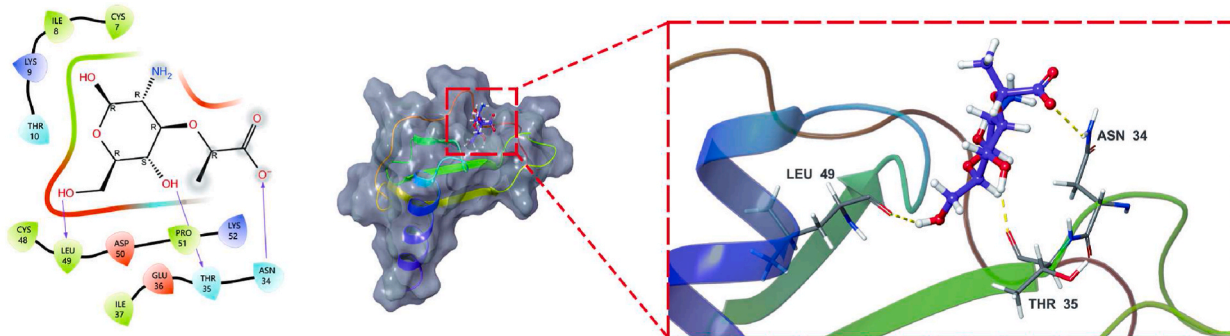


Fig. 10. The binding of muramic acid to the CXCL8 protein in both 2D and 3D formats.

PAEs, dimethyl phthalate (DMP), dihexyl phthalate (DnHP) and di (2-ethylhexane) phthalate (DEHP), to increase the resistance of biofilms to disinfectants [151].

Because of insufficient resources, our data volume is limited, and more repeated experiments are needed. Considering the noncarcinogenic risk of PAEs (hazard index, HI), the values for PAEs ranged from 3.72×10^{-7} and 7.89×10^{-4} [152]. Further experiments and data are required to confirm that the prevalence of PAEs is due to human involvement in the earth's ecological cycle following the extensive use of plastic products, or is it related to the coevolutionary strategy of plants and microorganisms [153,154], or both.

Therefore, in our results of bacterial rescue drug resistance, we had no way to eliminate the factors of PAEs. However, additional antibacterial ingredients are available among the tested volatile components, such as hexadecane, octadecane, and 3-ethyl-5-(2-ethyl-butyl)- [155]. We therefore postulate that this could be attributed to the combined action of several compounds.

In conclusion, the volatile compounds of MAPs demonstrated varying levels of effectiveness in combating bacterial drug resistance in the four bacterial strains we examined.

7.4. Transcriptomics and metabolomics experiments in drug-resistant *Staphylococcus aureus* results

The two Omics were compared to generate Venn diagrams that exhibit 22 overlapping pathways, as shown in Fig. 11.

The results of the correlation analysis and hierarchical clustering are displayed in Fig. 12. The figure displays the differential metabolites and genes of the group comparison along with their respective horizontal and vertical coordinates. Correlation coefficients are presented through the use of colour blocks, with red indicating positive correlation while blue indicating negative correlation. The strength of correlation is depicted through darker colours. Moreover, significant correlations have been denoted through plus signs ($+/++/+++ = p < 0.05/0.01/0.001$).

The co-expression data for the KEGG pathway was analysed using a combination of transcriptomics and metabolomics. Enrichment analyses were performed and bar graphs were used to illustrate the number of differentially expressed metabolites and genes involved in the KEGG pathway. The results are displayed in Fig. 13.

Table 7 provides comprehensive data on the co-expression disparities between the transcriptome and metabolome. Twenty-two pathways are highlighted in red due to their overlapping.

After conducting a search for the results, we have discovered the following information:

The genes upregulated in our experiment are inconsistent with previous experiments, with *adhE* in drug resistance [156] and *deoD*

Table 6
Antibacterial circle for drug resistance reversal experiment.

McFarland	Extractant co culture	<i>Staphylococcus aureus</i> , <i>S. aureus</i>		<i>Pseudomonas aeruginosa</i>		<i>Bacillus subtilis</i>		<i>Bacillus cereus</i>	
		1	3	1	1	1	1		
Drugs		Penicillin	Penicillin	streptomycin	Penicillin	streptomycin	Penicillin	streptomycin	
Blank control	0 h	10 mm (8 h)	0 mm (12 h)	11 mm (12 h)	0 mm (8 h)	18 mm (8 h)	0 mm (8 h)	14 mm (8 h)	
Dimethyl Phthalate (1:0.4)	24 h	14 mm (8 h)			0 mm (8 h)	16 mm (8 h)	0 mm (8 h)	18 mm (8 h)	
Dibutyl Phthalate (1:0.4)	24 h	12 mm (8 h)			0 mm (8 h)	14 mm (8 h)	0 mm (8 h)	14 mm (8 h)	
Diocetyl Phthalate (1:0.4)	24 h	10 mm (8 h)			0 mm (8 h)	13 mm (8 h)	0 mm (8 h)	11 mm (8 h)	
Diisooctyl Phthalate (1:0.4)	24 h	11 mm (8 h)			0 mm (8 h)	14 mm (8 h)	0 mm (8 h)	13 mm (8 h)	
Dimethyl Phthalate (1:0.2)	2 h		0 mm (12 h)	9 mm (12 h)					
Dibutyl Phthalate (1:0.2)	2 h		0 mm (12 h)	10 mm (12 h)					
Diocetyl Phthalate (1:0.2)	2 h		0 mm (12 h)	9 mm (12 h)					
Diisooctyl Phthalate (1:0.2)	2 h		0 mm (12 h)	9 mm (12 h)					
Dimethyl Phthalate (1:0.1)	3 h		0 mm (12 h)	9 mm (12 h)					
Dibutyl Phthalate (1:0.1)	3 h		0 mm (12 h)	8 mm (12 h)					
Diocetyl Phthalate (1:0.1)	3 h		0 mm (12 h)	7 mm (12 h)					
Diisooctyl Phthalate (1:0.1)	3 h		0 mm (12 h)	9 mm (12 h)					
1:1	3 h		0 mm (12 h)	14 mm (12 h)					
1:2	1 h		0 mm (12 h)	13 mm (12 h)					
1:4	24 h	23 mm (12 h)		Total death	0 mm (8 h)	21 mm (8 h)	0 mm (8 h)	19 mm (8 h)	
1 : 4-1 : 1	24 h	22 mm (8 h)							
1 : 4-1 : 1-1 : 1	24 h	16 mm (8 h)							
1 : 4-1 : 1-1 : 1-1 : 2	24 h	20 mm (8 h)							
1 : 4-1 : 1-1 : 1-1 : 2-None	24 h	14 mm (8 h)							
1:20	24 h				8 mm (8 h)	20 mm (8 h)	10 mm (8 h)	20 mm (8 h)	

*This diameter is the shortest resistance diameter of bacteria and extracts cultured in sterile EP tubes before the nutrient plate culture process, without adding any liquid.

[157] and MurA [158] in bacterial activity.

Consistent with previous experiments are the upregulation of *sdhA* [159] and *scrA* [160] in terms of drug resistance, the down-regulation of *mtlD* [161] in terms of bacterial activity.

The *sdhA* gene demonstrated the second most remarkable expression within 22 overlapping pathways. It exhibited co-expression with the upregulated phosphoenolpyruvate (PEP) in the TCA cycle, Carbon metabolism, Microbial metabolism in diverse environments, Metabolic pathways, as well as Biosynthesis of secondary metabolites five pathways. This gene plays a crucial role in the formation of biofilm [162].

PEP and *scrA* are co-expressed and upregulated together in the Phosphotransferase system (PTS). Experimental evidence suggests downregulation of bacterial EIIBC phosphotransferase components *scrA* and *mtlA* mediates drug resistance [160].

Although studies have shown that Mura's inhibitory effect leads to the accumulation of its matrix PEP, this substance is considered to be a carbon hunger signal [163]. It has been experimentally demonstrated that there is no greater expression of Mura in drug-resistant mutants than in wild-type strains, and that the heightened production of PEP is not connected to drug resistance but

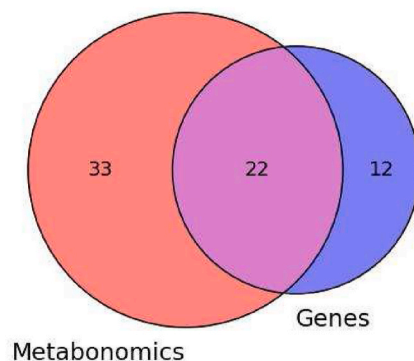


Fig. 11. Differential expression of pathways involved in Wayne diagrams in two omics.

instead to adjustments within the carbon metabolism of the bacterium, the diminished functionality of enzymes in the glycolysis pathway may be the root cause [164].

Our study discovered that Mura was upregulated. Additionally, the metabolomics analysis revealed that PEP was also upregulated in 14 pathway associations. As a result, drug resistance was reversed. Defective PEPCK activity has been demonstrated to cause drug resistance through PEP depletion. However, PEP supplementation considerably reduces both antibiotic-induced persister formation and drug resistance mutations [165]. Our experiment's outcomes are corroborated by these findings.

Furthermore, PEP is an immunomodulatory compound that inhibits T helper (Th) 17 cells differentiation and inhibits interleukin (IL)-17A. PEP supplementation to mice externally inhibits autoimmune diseases [166].

Interestingly, our research discovered that *uhpT*, *agrB*, *agrC*, and *agrA* were expressed at lower levels, and acetoacetate was expressed at higher levels as a result of co-expression in the two-component system. Only the expression of *agrB*, *agrC*, and *agrA* was reduced regarding quorum sensing. Some studies indicate that decreased expression of UhpT enhances bacterial drug resistance, while sensitivity of *S. aureus* strains to antimicrobial agents is regulated via a two-component signalling pathway [167]. Inactivation of *agrB*, *agrC*, *agrA* increases resistance through thickening of biofilm [168] but reduces virulence [169]. However, other studies have shown that significant antibiofilm activity is associated with the downregulation of *agrB*, *agrC*, and *agrA* [170]. Experiments conducted on mice showed that the biofilm thickened with targeted *agrAC* cells, but these cells did not develop any resistance [171].

Given the complex mechanisms of drug resistance [172]. Our results indicate that bacterial resistance cannot be attributed to a single gene or metabolite. The combined mutations in *sdhA*, *scrA*, and PEP effectively improved drug resistance in our experiments.

Significantly, upregulation of *groEL* solely in transcriptome differentially expressed genes can induce PTX3 production by nuclear factor-kappa B (NF- κ B) activation [173]. This affects the body's innate immunity and reduces lung infections caused by bacteria [174]. AKT and NF- κ B are both essential for activating PTX3 [175]. In our network pharmacology experiments, AKT1 emerged as the primary target, supported by the potential of transcriptomic *groEL* mutations to indirectly affect the human body in rescue drug-resistance experiments, ultimately pointing to the same target.

It is worth mentioning that the *Staphylococcus aureus* employed in our study was sourced from the nasal cavity of seven-year-old children. The reduction of *Staphylococcus aureus* could potentially slow down the deterioration of lung function and decrease tissue damage in mice [176].

8. Discuss

Given the complexity of mind-body relationships [177], the interaction between the nervous system and cancer [178], plants face corresponding drought through the modulation of monoterpene emissions [179], possible mucosal immunity [180], reduction in human-induced aerosol emissions results in an imbalanced distribution of precipitation resources [181], BVOCs and interactions with bacteria and viruses, and other variables. It is possible that humans made a misstep when we started building cities in the past, leading us to remove vital symbiotic species from our daily lives. This may have contributed to the worsening of human diseases and the natural environment. Consequently, we are compelled to reassess the connection between humanity and the environment, and the crucial role of MAPs in ecosystems. However, thankfully, we have now recognized their immense potential and developed novel methods of utilizing them.

In the course of the APEHE experiment, we found many other interesting and thought-provoking phenomena. Of course, there is still much confusion about this, for example, the biological role of most terpenes is unknown [182]. The effects and pathways of carbon enrichment in greenhouse environments and field environments are not clear enough [183]. There are insufficient data on the relationship threshold interval between essential oils, fungi and soil [184]. The comprehension of the synergistic, antagonistic, and airborne recombination of volatiles from naturally grown plants is limited, as is the toxicological safety data. Synthetic compounds, such as paracetamol and flurbiprofen, are known to form in the environment of APEHE, the mechanisms of their formation are not well understood. Whether MAPs can grow and volatilise organic compounds better in which materials, e.g., a more energy-efficient building environment [185].

At the application level, the interaction between plants and the environment is not like many experiments that can be precisely

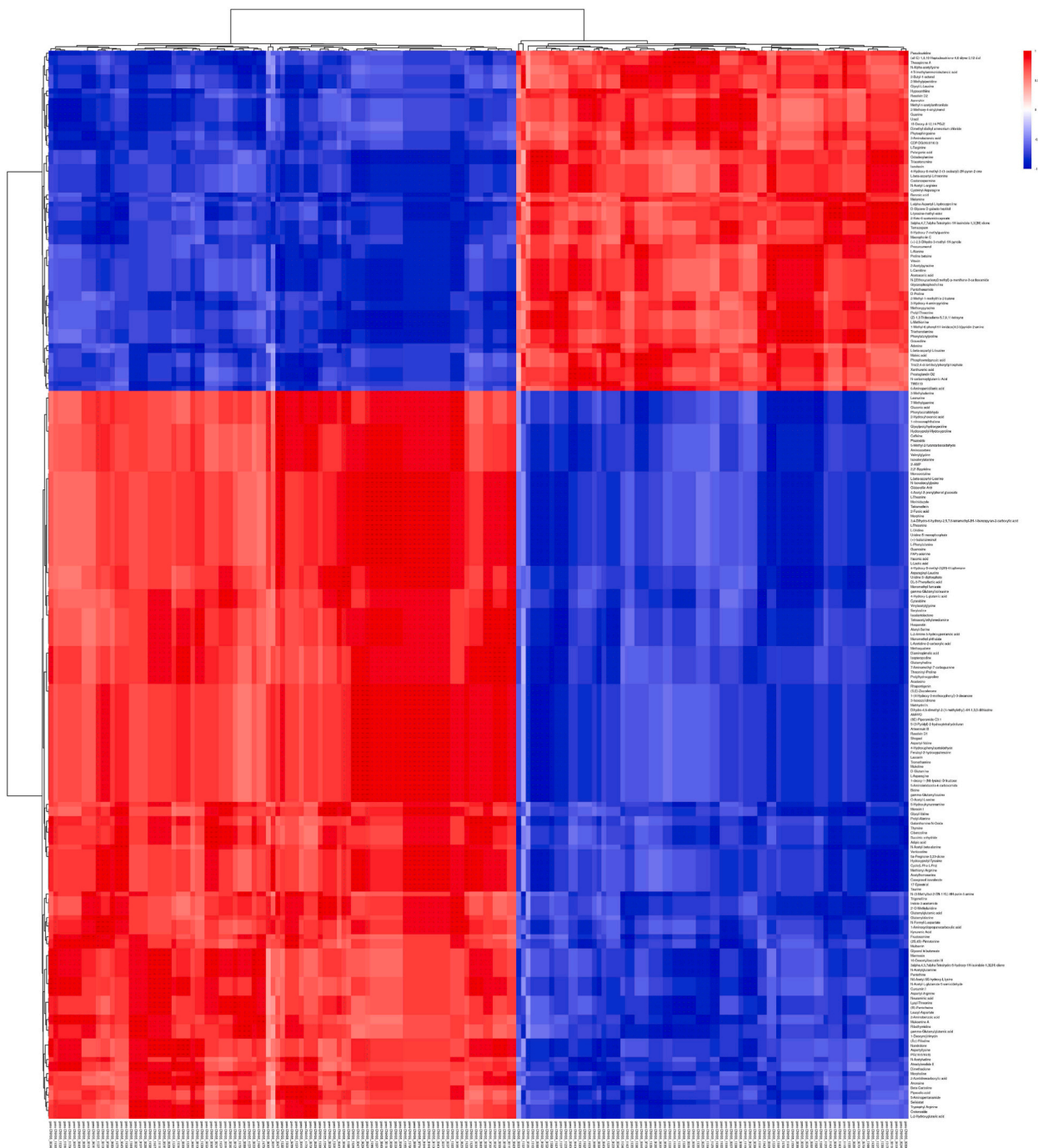


Fig. 12. Correlation analysis hierarchical clustering heatmap.

quantified, with high complexity, high activity and unstable compounds. There are still many problems to be solved to achieve some degree of dynamic equilibrium.

In our research, it was found that some of the required plants were not easily obtainable in the market. Furthermore, certain available plants were grown for ornamental purposes in gardens and lacked the essential aromatic content. For example, unscented varieties of cypresses and *Crossostephium chinense* had reduced odour variation and volatility due to excessive pesticide use. These factors made the research process considerably more challenging. This statement emphasises the significance of balancing the functionality of plants in the environment with aesthetics.

There are some limitations to consider:

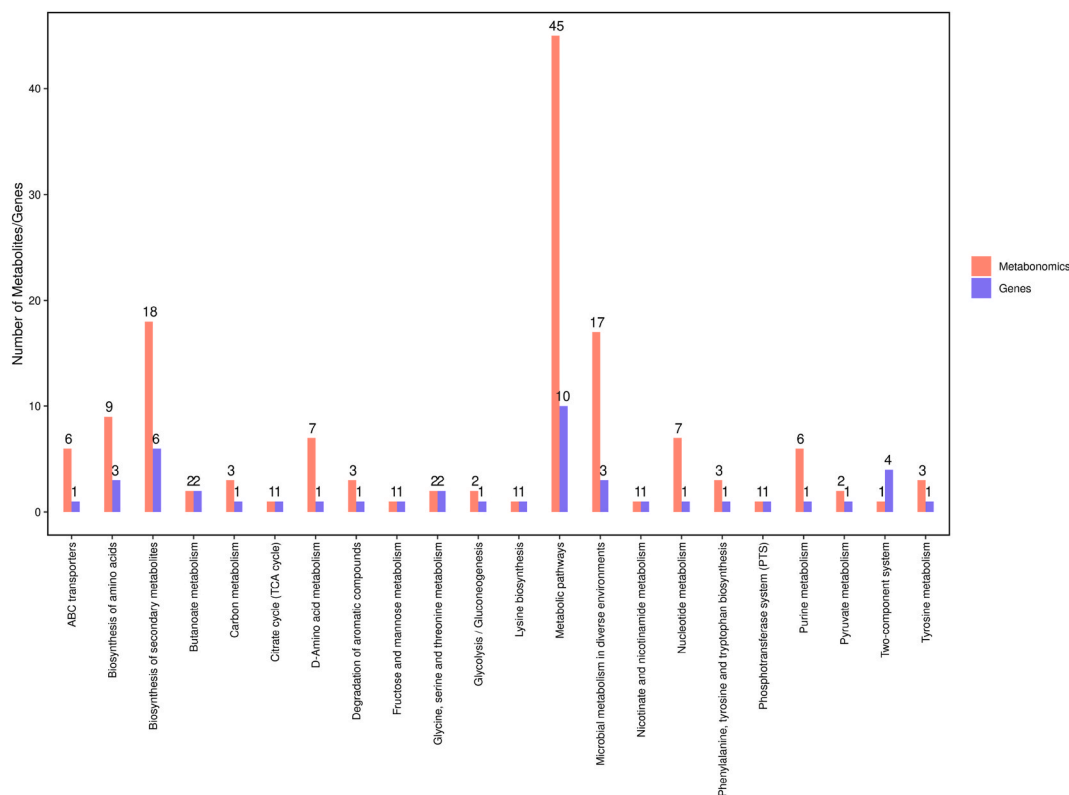


Fig. 13. KEGG pathway annotation comparison histogram.

Experimental Methods In regards to the direct effects of the compound components on the human body, we conducted network pharmacology and molecular docking. That is insufficient. However, further experiments are required to verify the specific effects of these compounds on the human body after entering through the respiratory tract. When resources allow, it is crucial to examine these effects from various angles.

Further optimisation is required for the experimental methods used to determine the composition of compounds in the air. The extracted compositions may differ from the actual air substance composition due to the varying polarity of solvents. Moreover, there may be differences between compounds routinely collected directly from plant tissues and those that are volatilized into the air through natural growth of the plant after oxidation and light exposure.

In regard to optimising and enriching the production and volatilisation of effective secondary metabolites from plants in the environment, for different regions and scenarios, different perspectives of thinking may require different species and efficacies, and structural models designed from different perspectives are bound to be different, with issues such as compositional research, species selection, planting methods, species modification techniques and continuous monitoring of organic compounds in the air requiring more researchers from different fields to anticipate working together to design structures and models suitable for different cities and environments.

It is worth exploring in depth the possibility of new avenues in APEHE for other research directions. For instance:

Whether increased PEP in APEHE-treated microbes impacts respiratory immunity is a worthy expansion of this avenue of research. Meanwhile, whether carbon hunger signals can indicate that bacteria treated with APEHE are engaging in more carbon sequestration is also a direction worth exploring in depth.

In the cross-referenced pathway 'Biosynthesis of Secondary Metabolites', 6 genes were up-regulated and 18 metabolites differed, including Morphine, Caffeine, and the potentially anti-tumour valuable Marmesin [186]. This may provide new ideas for using bacteria to produce specific compounds.

At the same time, as aerosols endure in the atmosphere for protracted periods, may also affect antibiotic resistance genes (ARGs) in clouds [187], preventing the spread of bacterial resistance through the global water cycle. We may have found a technique to generally revive the capacity for wild antibiotic-sensitive flora in the natural environment [188].

The prevalence of polycyclic aromatic hydrocarbons (PAHs) in the universe [189] forms larger PAHs from small molecules in the discharge [190], and a combination of biochar and oxalic acid could improve the bacterial degradation of PAHs in soil [191]. Whether the connection between these factors could open up more possibilities for new perspectives in our search for questions about the origin of life [192], etc. These findings may lead to further research and the identification of new areas of overlap.

With the maturity of the various models of aromatic environmental engineering, whether we can adapt them to other planets is also

Table 7
Detailed data on strongly correlated differential co-expression and pathways in the transcriptome and metabolome.

ID	Description	genes	Compounds (dem)
sau05150	Staphylococcus aureus infection	spa↑ clfB↑	
sau00300	Lysine biosynthesis	lysA↑	C00666
sau00470	D-Amino acid metabolism	lysA↑	C00763;C00041;C00079;C00073;C00819;C00188;C00666
sau01100	Metabolic pathways	lysA↑ deoD↑ adhE↑ sdhA↑ trpA↑ murA↑ mtID↓ hutU↓ betA↓ hisH↑	C02376;C00763;C00074;C00490;C00186;C01367;C00408;C00041;C00696;C02067;C00242;C00106;C01181;C00387;C00079;C0073;C12144;C00147;C00262;C00105;C04051;C01384;C16675;C00245;C00601;C00152;C06104;C00257;C00180;C00990;C03196;C00819;C00188;C01888;C00108;C03765;C01516;C01546;C00015;C00164;C07481;C01250;C05548;C05638;C00666
sau01110	Biosynthesis of secondary metabolites	lysA↑ deoD↑ adhE↑ sdhA↑ trpA↑ hisH↑	C00074;C00186;C00408;C00041;C00079;C00073;C00147;C00152;C00257;C00180;C00188;C00108;C03765;C01516;C07481;C01250;C09276;C00666
sau01120	Microbial metabolism in diverse environments	lysA↑ adhE↑ sdhA↑	C00074;C00186;C00408;C00041;C01384;C00601;C06104;C00257;C00180;C00990;C03196;C00188;C00108;C01546;C00164;C07481;C00666
sau01230	Biosynthesis of amino acids	lysA↑ trpA↑ hisH↑	C00074;C00041;C00079;C00073;C00152;C00188;C00108;C01250;C00666
sau00230	Purine metabolism	deoD↑	C01367;C00242;C00387;C00147;C00262;C04051
sau00760	Nicotinate and nicotinamide metabolism	deoD↑	C01384
sau01232	Nucleotide metabolism	deoD↑	C00242;C00106;C00387;C00147;C00262;C00105;C00015
sau00010	Glycolysis / Gluconeogenesis	adhE↑	C00074;C00186
sau00071	Fatty acid degradation	adhE↑	
sau00350	Tyrosine metabolism	adhE↑	C01384;C03765;C00164
sau00620	Pyruvate metabolism	adhE↑	C00074;C00186
sau00625	Chloroalkane and chloroalkene degradation	adhE↑	
sau00626	Naphthalene degradation	adhE↑	
sau00650	Butanoate metabolism	adhE↑ sdhA↑	C01384;C00164
sau01220	Degradation of aromatic compounds	adhE↑	C06104;C00180;C00108
sau02010	ABC transporters	msmX↓	C00041;C01181;C00387;C00079;C00245;C00188
sau02020	Two-component system	uhpT↓ agrB↓ agrC↓ agrA↓	C00164
sau02024	Quorum sensing	sspA↓ hhd↓ agrB↓ agrC↓ agrA↓	
sau00020	Citrate cycle (TCA cycle)	sdhA↑	C00074
sau00190	Oxidative phosphorylation	sdhA↑	
sau01200	Carbon metabolism	sdhA↑	C00074;C00041;C00257
sau00260	Glycine, serine and threonine metabolism	trpA↑ betA↓	C00188;C01888
sau00400	Phenylalanine, tyrosine and tryptophan biosynthesis	trpA↑	C00074;C00079;C00108
sau03018	RNA degradation	dnaK↑ groEL↑	
sau00520	Amino sugar and nucleotide sugar metabolism	murA↑	
sau00550	Peptidoglycan biosynthesis	murA↑	
sau01250	Biosynthesis of nucleotide sugars	murA↑	
sau00051	Fructose and mannose metabolism	mtID↓	C00186
sau00340	Histidine metabolism	hutU↓ hisH↑	
sau00500	Starch and sucrose metabolism	scrA↑	
sau02060	Phosphotransferase system (PTS)	scrA↑	C00074

one of the directions in which we can try to continue research and development.

It is important to note that although APEHE has many potential benefits, it does not mean that it can replace existing strategies to attenuation and elimination of airborne microorganisms in the environment, energy transition, environmental measures, carbon neutral programme, biodiversity pursuits, etc., but rather that APEHE can complement many existing strategies and help us to achieve our desired goals better and faster.

At the same time, from the perspective of the circular economy [193], from the perspective of mental and physical health of the whole social group, biomedicine, ecological environment, energy structure optimisation and even the transformation of other planets, APEHE has enough potential value and significance. APEHE has the potential to become a leverage point of the Earth system and to cause a positive chain reaction. Although we are still far from these mature models, we believe that through scientific and rigorous research and demonstration, all of humanity can work together to find the right way for each participant in our planet's ecosystem to have a more harmonious path.

It is hoped that APEHE's potential will improve the lives of all human beings in the future.

9. Conclusion

Our experiments demonstrate that atmospheric APEHE organic volatiles primarily reduce bacterial drug resistance through combined mutations in *sdhA*, *scrA*, and *PEP*. Additionally, these volatiles have the potential to affect immunity through bacterial exposure in the nasal cavity and mitigate the deleterious effects of *AKT1* hyperactivation. Meanwhile, the network pharmacology and molecular binding results showed that *AKT1* is the primary target, and *MMP9* and *TLR4* are secondary targets. This is in agreement with the results of the rescue bacterial resistance assay. *AKT1* has great therapeutic potential in the fields of broad-spectrum antiviral therapies, respiratory diseases, and cancer, and is widely distributed in the human body. We demonstrate that APEHE has direct and indirect effects on human health.

However, relying exclusively on network pharmacology and molecular docking to demonstrate the interaction between optimised airborne compounds and the human body has limitations. Further research is necessary to confirm the mechanism. Additionally, more experiments are required to determine whether the bacteria in the human respiratory tract are as effective as *in vitro* experiments in reversing drug resistance in treated bacteria.

The APEHE system has the potential to offer numerous benefits, including enhanced sequestration of carbon and nitrogen. It can also cool the planet by increasing low-level cloud systems. Additionally, it has the potential to affect human physical and mental health through compounds in aerosols, reversing microbial resistance, and limiting airborne pathogens. Supporting interdisciplinary technologies, such as terpene energy production, is aimed at establishing a sustainable circular economy and generating additional economic benefits through urban restructuring. The text provides innovative perspectives for other disciplines, such as exploring the potential habitability of celestial bodies. This approach has the potential to become a leverage point for the Earth system, and a new research direction has been established.

Therefore, MAPs should not only be cultivated for drug extraction in fields. They have a complex and inseparable relationship with microorganisms, insects, and even the spread of infectious diseases, the natural climate, and the physical and mental health of human beings. To reintroduce MAPs into urban and natural environments, it is crucial to consider scientifically appropriate methods and formulations. It is also important to develop different models for varying environments and needs.

In summary, this text addresses the various potentials of APEHE from different perspectives and experimentally demonstrates its potential impact on human health and importance.

Funding sources

All funding sources are provided by the author herself and the author's company HEFEI XIAODOUKOU HEALTH TECH CO LTD.

Ethics approval and consent to participate

Not applicable.

CRedit authorship contribution statement

MengYu Lu: Writing – review & editing, Writing – original draft, Validation, Supervision, Software, Resources, Project administration, Methodology, Investigation, Funding acquisition, Formal analysis, Data curation, Conceptualization.

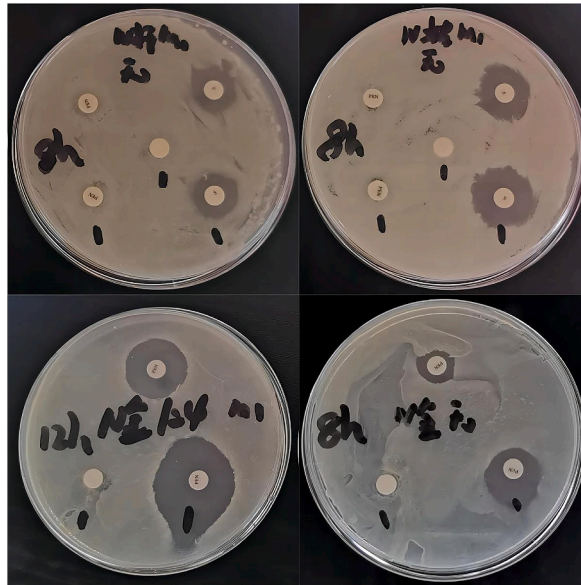
Declaration of competing interest

The authors declare the following financial interests/personal relationships which may be considered as potential competing interests: MengYu Lu has patent #CN111937664B licensed to HEFEI XIAODOUKOU HEALTH TECH CO LTD. If there are other authors, they declare that they have no known competing financial interests or personal relationships that could have appeared to influence the work reported in this paper.

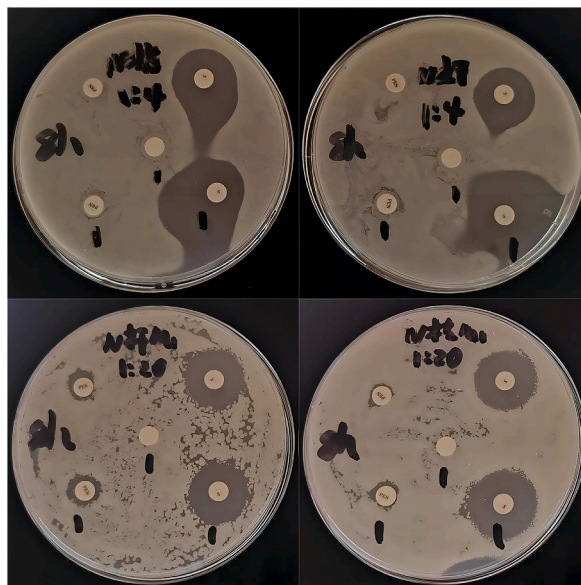
Acknowledgements

The author received much support in the process of doing this work. It is very grateful to the predecessors who have done much preliminary work in various fields, HelixLife, Swarna Club, Li Fuming doctor of traditional Chinese medicine and Dr. Ren Peng for inspiration and guidance in my scientific research work, and my family and friends for their support. Special thanks to my closest friend Mr. Zhu Yilong, and “Xiaolongbao” for their companionship, support, and encouragement. Without them, it would be difficult for me to persist in completing this work. Finally, I would like to express my gratitude to “Gaia” and the plants for their dedication and sacrifice to the Earth, especially those I have planted to death.

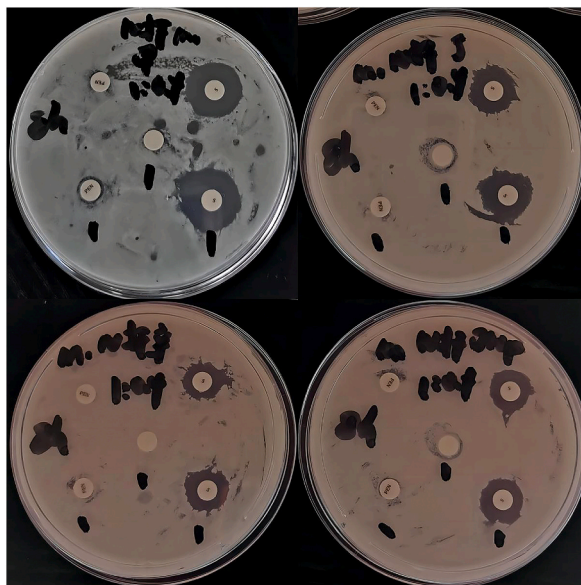
Appendix 1



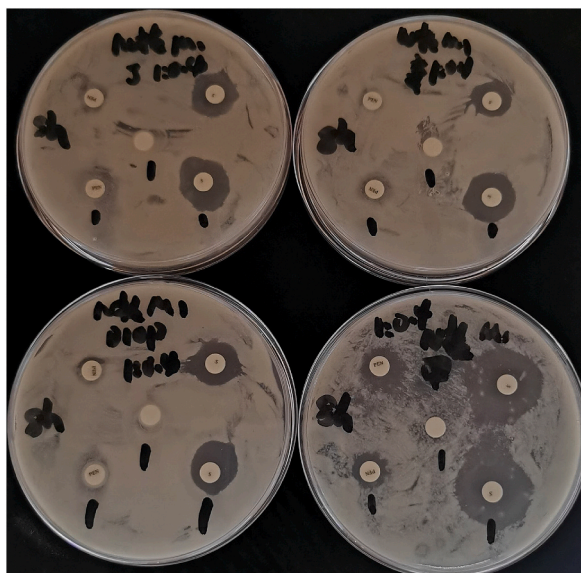
Bacillus cereus, *Bacillus subtilis*, *Staphylococcus aureus* Blank control P24-8 and *Staphylococcus aureus* 1:4 P24-12.



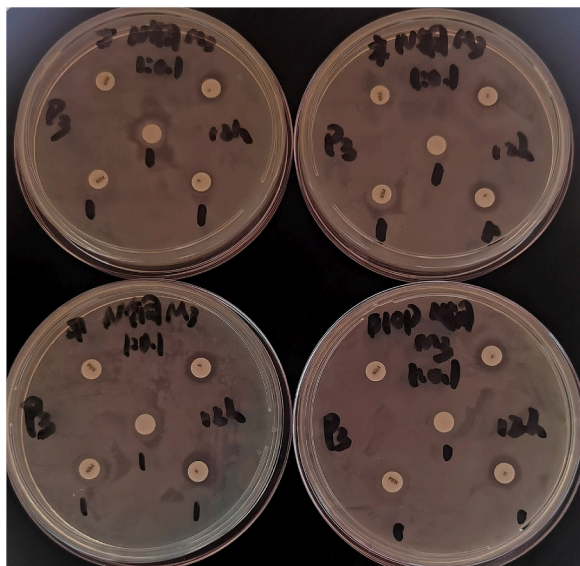
Bacillus cereus, *Bacillus subtilis* 1:4 and 1:20 P24-8.



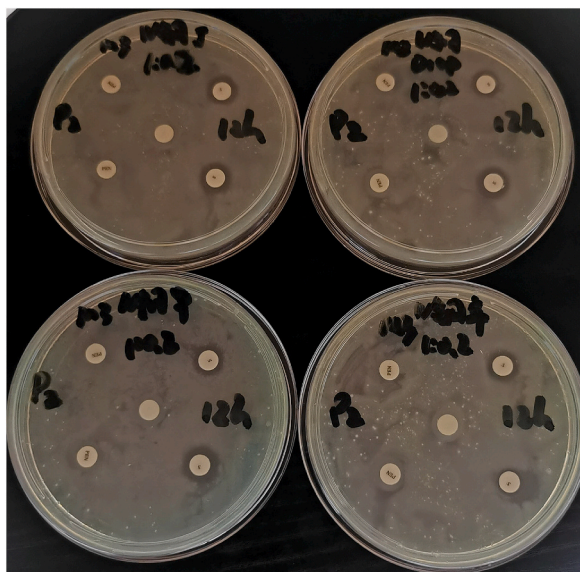
Bacillus cereus PAEs 1:0.4 P24-8.



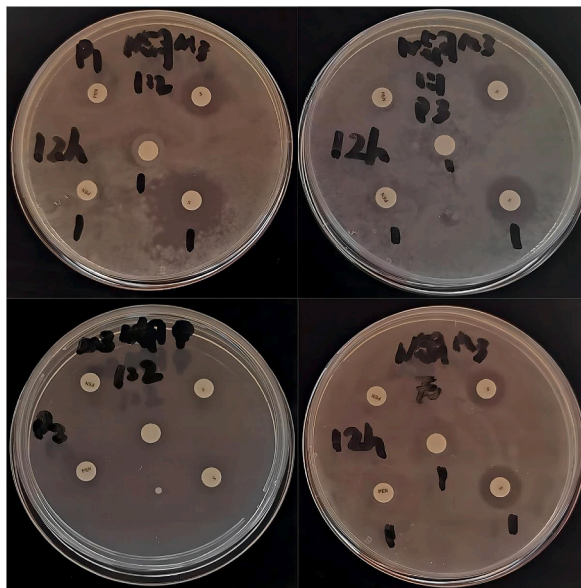
Bacillus subtilis PAEs 1:0.4 P24-8



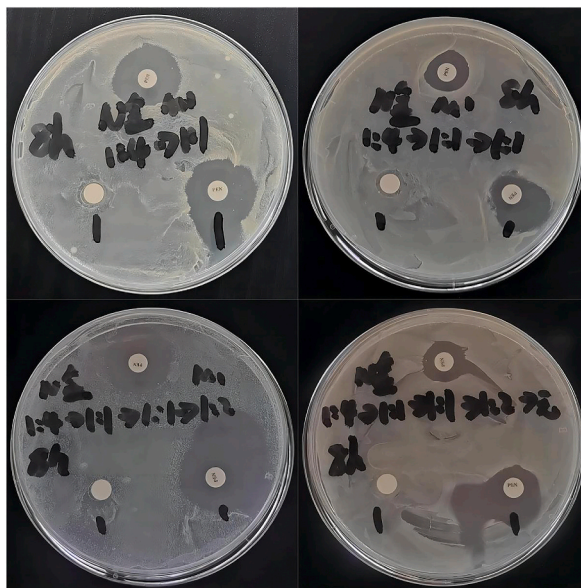
Pseudomonas aeruginosa PAEs 1:0.1 P3-12.



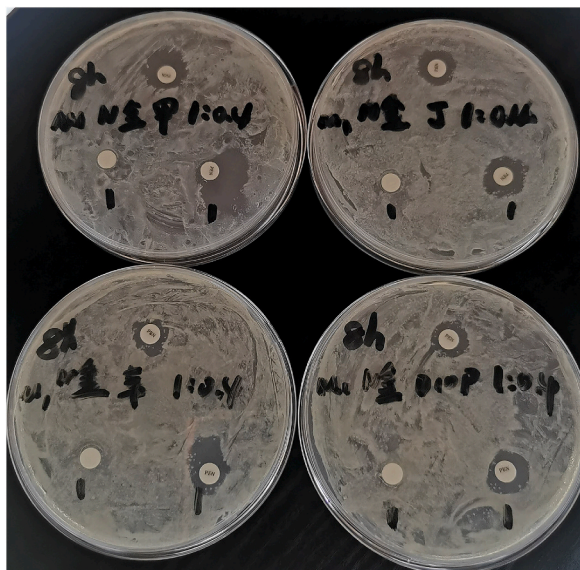
Pseudomonas aeruginosa PAEs 1:0.2 P2-12.



Pseudomonas aeruginosa 1:2 P1-12 and 1:1 P3-12 and 1:2 P2-12 and Blank control.



Staphylococcus aureus 1: 4–1:1 and 1:4–1:1–1:1 and 1:4–1:1-1:1–1:2 and 1:4–1:1-1:1-1:2-None P24-8.



Staphylococcus aureus PAEs 1:0.4 P24-8.

References

- [1] J. Kroymann, Natural diversity and adaptation in plant secondary metabolism, *Curr. Opin. Plant Biol.* 14 (3) (2011) 246–251, <https://doi.org/10.1016/j.pbi.2011.03.021>.
- [2] J.L. Berini, S.A. Brockman, A.D. Hegeman, P.B. Reich, R. Muthukrishnan, R.A. Montgomery, J.D. Forester, Combinations of abiotic factors differentially alter production of plant secondary metabolites in five woody plant species in the boreal-temperate transition zone, *Front. Plant Sci.* 9 (2018) 1257, <https://doi.org/10.3389/fpls.2018.01257>.
- [3] Shikha Srivastava, Saurabh Srivastava, Manju Rawat Singh, Deependra Singh, Babu L. Tekwani, Chapter 11 - novel perspectives for delivery of bioactives through blood–brain barrier and treatment of brain diseases, in: Manju Rawat Singh, Deependra Singh, Jagat R. Kanwar, Nagendra Singh Chauhan (Eds.), *Advances and Avenues in the Development of Novel Carriers for Bioactives and Biological Agents*, Academic Press, 2020, pp. 317–341, <https://doi.org/10.1016/B978-0-12-819666-3.00011-0>. ISBN 9780128196663.
- [4] O. Menzibeya, Welcome, Blood brain barrier inflammation and potential therapeutic role of phytochemicals, *PharmaNutrition* 11 (2020) 100177, <https://doi.org/10.1016/j.phanu.2020.100177>. ISSN 2213-4344.
- [5] Walaa M.S. Ahmed, Naglaa M. Abdel-Azeem, Marwa A. Ibrahim, Nermeen A. Helmy, Abeer M. Radi, Neuromodulatory effect of cinnamon oil on behavioural disturbance, CYP1A1, iNOS transcripts and neurochemical alterations induced by deltamethrin in rat brain, *Ecotoxicol. Environ. Saf.* 209 (2021) 111820, <https://doi.org/10.1016/j.ecoenv.2020.111820>. ISSN 0147-6513.
- [6] C.C. Wen, Y.H. Kuo, J.T. Jan, et al., Specific plant terpenoids and lignoids possess potent antiviral activities against severe acute respiratory syndrome coronavirus, *J. Med. Chem.* 50 (17) (2007) 4087–4095, <https://doi.org/10.1021/jm070295s>.
- [7] V. De Luca, V. Salim, S.M. Atsumi, F. Yu, Mining the biodiversity of plants: a revolution in the making, *Science* 336 (2012) 1658–1661, <https://doi.org/10.1126/science.1217410>.
- [8] E.T. Wurtzel, T.M. Kutchan, Plant metabolism, the diverse chemistry set of the future, *Science* 353 (2016) 1232–1236, <https://doi.org/10.1126/science.aad2062>.
- [9] G.A. Cordell, Biodiversity and drug discovery — a symbiotic relationship, *Phytochemistry* 55 (6) (2000) 463–480, [https://doi.org/10.1016/S0031-9422\(00\)00230-2](https://doi.org/10.1016/S0031-9422(00)00230-2).
- [10] Tiantian Lin, Klaas Vrieling, Diane Laplanche, Peter G.L. Klinkhamer, Yonggen Lou, Leon Bekooij, Thomas Degen, Carlos Bustos-Segura, Ted C.J. Turlings, Gaylord A. Desurmont, Evolutionary changes in an invasive plant support the defensive role of plant volatiles, *Curr. Biol.* 31 (15) (2021) 3450–3456, <https://doi.org/10.1016/j.cub.2021.05.055>, e5, ISSN 0960-9822.
- [11] V. Mani, S. Park, J.A. Kim, S.I. Lee, K. Lee, Metabolic perturbation and synthetic biology strategies for plant terpenoid production—an updated overview, *Plants* 10 (10) (2021 Oct 14) 2179, <https://doi.org/10.3390/plants10102179>. PMID: 34685985; PMCID: PMC8539415.
- [12] I.F. González Mera, et al., Secondary metabolites in plants: main classes, phytochemical analysis and pharmacological activities, *Bionatura* 4 (4) (2019) 1000–1009, <https://doi.org/10.21931/RB/2019.04.04.11>.
- [13] J. Gershenzon, N. Dudareva, The function of terpene natural products in the natural world, *Nat. Chem. Biol.* 3 (7) (2007) 408–414.
- [14] O. Musidlak, R. Nawrot, A. Goździcka-Józefiak, Which plant proteins are involved in antiviral defense? Review on in vivo and in vitro activities of selected plant proteins against viruses, *Int. J. Mol. Sci.* 18 (11) (2017) 2300, <https://doi.org/10.3390/ijms18112300>.
- [15] S. Prabuseenivasan, M. Jayakumar, S. Ignacimuthu, In vitro antibacterial activity of some plant essential oils, *BMC Compl. Alternative Med.* 6 (1) (2006) 1–8.
- [16] A. Elaissi, Z. Rouis, N.A.B. Salem, et al., Chemical composition of 8 eucalyptus species' essential oils and the evaluation of their antibacterial, antifungal and antiviral activities, *BMC Compl. Alternative Med.* 12 (2012) 81, <https://doi.org/10.1186/1472-6882-12-81>.
- [17] P. Schnitzler, et al., Susceptibility of drug-resistant clinical herpes simplex virus type 1 strains to essential oils of ginger, thyme, hyssop, and sandalwood, *Antimicrob. Agents Chemother.* 51 (5) (2007) 1859–1862.
- [18] R. Naveed, I. Hussain, A. Tawab, et al., Antimicrobial activity of the bioactive components of essential oils from Pakistani spices against *Salmonella* and other multi-drug resistant bacteria, *BMC Compl. Alternative Med.* 13 (2013) 265, <https://doi.org/10.1186/1472-6882-13-265>.

- [19] W.L. Lai, H.S. Chuang, M.H. Lee, C.L. Wei, C.F. Lin, Y.C. Tsai, Inhibition of herpes simplex virus type 1 by thymol-related monoterpenoids, *Planta Med.* 78 (15) (2012) 1636–1638.
- [20] P. Schnitzler, K. Schön, J. Reichling, Antiviral activity of Australian tea tree oil and eucalyptus oil against herpes simplex virus in cell culture, *Pharmazie* 56 (2001) 343–347.
- [21] A. Schuhmacher, J. Reichling, P. Schnitzler, Virucidal effect of peppermint oil on the enveloped viruses herpes simplex virus type 1 and type 2 in vitro, *Phytomedicine* 10 (2003) 504–510.
- [22] J. Reichling, C. Koch, E. Stahl-Biskup, C. Sojka, P. Schnitzler, Virucidal activity of a beta-triketone-rich essential oil of *Leptospermum scoparium* (manuka oil) against HSV-1 and HSV-2 in cell culture, *Planta Med* 71 (2005) 1123–1127.
- [23] R. Boubaker-Elandalousi, et al., Non-cytotoxic *Thymus capitata* extracts prevent Bovine herpesvirus-1 infection in cell cultures, *BMC Vet. Res.* 10 (1) (2014) 231.
- [24] S. Mediouni, et al., Oregano oil and its principal component carvacrol inhibit HIV-1 fusion into target cells, *J. Virol. JVI* (2020), 00147-00120.
- [25] M. Loizzo, A. Saab, R. Tundis, G. Statti, F. Menichini, I. Lampronti, R. Gambari, J. Cinatl, H. Doerr, Phytochemical analysis and in vitro antiviral activities of the essential oils of seven Lebanon species, *Chem. Biodivers.* 5 (2008) 461–470, <https://doi.org/10.1002/cbdv.200890045>.
- [26] Y.M. Siddiqui, M. Ettayebi, A.M. Haddad, M.N. Al-Ahdal, Effect of essential oils on the enveloped viruses: antiviral activity of oregano and clove oils on herpes simplex virus type 1 and Newcastle disease virus, *Med. Sci. Res.* 24 (1996) 185–186.
- [27] X. Huang, Y. Gao, F. Xu, et al., Molecular mechanism underlying the anti-inflammatory effects of volatile components of *Ligularia fischeri* (Ledeb) Turcz based on network pharmacology, *BMC Complement Med Ther* 20 (2020) 109, <https://doi.org/10.1186/s12906-020-2855-3>.
- [28] Tariq S. Tariq, S. Wani, W. Rasool, K. Shafi, M.A. Bhat, A. Prabhakar, A.H. Shalla, M.A. Rather, A comprehensive review of the antibacterial, antifungal and antiviral potential of essential oils and their chemical constituents against drug-resistant microbial pathogens, *Microb. Pathog.* 134 (2019 Sep) 103580, <https://doi.org/10.1016/j.micpath.2019.103580>. Epub 2019 Jun 11. PMID: 31195112.
- [29] Raphaelle Sousa Borges, Brenda Lorena Sánchez Ortiz, Arlindo César Matias Pereira, Hady Keita, José Carlos Tavares Carvalho, Rosmarinus officinalis essential oil: a review of its phytochemistry, anti-inflammatory activity, and mechanisms of action involved, *J. Ethnopharmacol.* 229 (2019) 29–45, <https://doi.org/10.1016/j.jep.2018.09.038>. ISSN 0378-8741.
- [30] G. Horváth, K. Ács, Essential oils in the treatment of respiratory tract diseases highlighting their role in bacterial infections and their anti-inflammatory action: a review, *Flavour Fragrance J.* 30 (2015) 331–341, <https://doi.org/10.1002/ffj.3252>.
- [31] K. Ács, V.L. Balázs, B. Kocsis, et al., Antibacterial activity evaluation of selected essential oils in liquid and vapor phase on respiratory tract pathogens, *BMC Compl. Alternative Med.* 18 (2018) 227, <https://doi.org/10.1186/s12906-018-2291-9>.
- [32] Evgeny V. Usachev, Oleg V. Pyankov, Olga V. Usacheva, Igor E. Agranovski, Antiviral activity of tea tree and eucalyptus oil aerosol and vapour, *J. Aerosol Sci.* 59 (2013) 22–30, <https://doi.org/10.1016/j.jaerosci.2013.01.004>. ISSN 0021-8502.
- [33] Panikar Sukanya, Gunasekaran Shoba, Muthukrishnan Arun, Joseph Sahayarayan Jesudass, A. Usha Raja Nanthini, Chinnathambi Arunachalam, Sulaiman A. Alharbi, Omaiya Nasif, Hak-Jae Kim, Essential oils as an effective alternative for the treatment of COVID-19: molecular interaction analysis of protease (Mpro) with pharmacokinetics and toxicological properties, *Journal of Infection and Public Health* 14 (5) (2021) 601–610, <https://doi.org/10.1016/j.jiph.2020.12.037>. ISSN 1876-0341.
- [34] Yali Yuan, Zhihong Sun, Astrid Kännaste, Ming Guo, Guomo Zhou, Ülo Niinemets, Isoprenoid and aromatic compound emissions in relation to leaf structure, plant growth form and species ecology in 45 East-Asian urban subtropical woody species, *Urban For. Urban Green.* 53 (2020) 126705, <https://doi.org/10.1016/j.ufug.2020.126705>. ISSN 1618-8667.
- [35] Y. Fujiwara, M. Ito, Synergistic effect of fragrant herbs in Japanese scent sachets, *Planta Med.* 81 (3) (2015 Feb) 193–199, <https://doi.org/10.1055/s-0034-1396138>. Epub 2015 Feb 11. PMID: 25671383.
- [36] J.-F. Bastin, et al., The global tree restoration potential, *Science* 365 (6448) (2019) 76–79.
- [37] Godwin Leslie Muhati, Daniel Olago, Lydia Olaka, Quantification of carbon stocks in Mount Marsabit Forest Reserve, a sub-humid montane forest in northern Kenya under anthropogenic disturbance, *Global Ecology and Conservation* 14 (2018) e00383, <https://doi.org/10.1016/j.gecco.2018.e00383>. ISSN 2351-9894.
- [38] Peiyuan Li, Zhi-Hua Wang, Environmental co-benefits of urban greening for mitigating heat and carbon emissions, *J. Environ. Manag.* 293 (2021) 112963, <https://doi.org/10.1016/j.jenvman.2021.112963>. ISSN 0301-4797.
- [39] Mari Ariluoma, Juudit Ottelein, Ranja Hautamäki, Eeva-Maria Tuukkanen, Miia Mänttari, Carbon sequestration and storage potential of urban green in residential yards: a case study from Helsinki, *Urban For. Urban Green.* 57 (2021) 126939, <https://doi.org/10.1016/j.ufug.2020.126939>. ISSN 1618-8667.
- [40] R. Erfanzadeh, B. Bahrami, J. Motamedi, J. Pétilion, Changes in soil organic matter driven by shifts in co-dominant plant species in a grassland, *Geoderma* 213 (2014) 74–78, <https://doi.org/10.1016/j.geoderma.2013.07.027>.
- [41] K. Dosso, B.B. N'guessan, A.P. Bidie, B.N. Ngangoran, S. Méité, D. N'guessan, A.P. Yapo, E.E. Ehilé, Antidiarrhoeal activity of an ethanol extract of the stem bark of *Piliostigma reticulatum* (Caesalpinaceae) in rats, *Afr. J. Tradit., Complementary Altern. Med.* 9 (2) (2011 Dec 29) 242–249, <https://doi.org/10.4314/ajtcam.v9i2.9>. PMID: 23983341; PMCID: PMC3746628.
- [42] M.B.H. Bright, I. Diedhiou, R. Bayala, K. Assigbetse, L. Chapuis-Lardy, Y. Ndour, R.P. Dick, Long-term *Piliostigma reticulatum* intercropping in the Sahel: crop productivity, carbon sequestration, nutrient cycling, and soil quality, *Agric. Ecosyst. Environ.* 242 (2017) 9–22, <https://doi.org/10.1016/j.agee.2017.03.007>.
- [43] M. Kuypers, H. Marchant, B. Kartal, The microbial nitrogen-cycling network, *Nat. Rev. Microbiol.* 16 (2018) 263–276, <https://doi.org/10.1038/nrmicro.2018.9>.
- [44] Colin Goldblatt, Mouterde Claire, Timothy Lenton, Adrian Matthews, Andrew Watson, Kevin Zahnle, Nitrogen-enhanced greenhouse warming on early Earth, *Nat. Geosci.* 2 (2009) 891–896, <https://doi.org/10.1038/ngeo692>.
- [45] Xinxin Chen, Beizhou Song, Yuncong Yao, Hongying Wu, Jinghui Hu, Lingling Zhao, Aromatic plants play an important role in promoting soil biological activity related to nitrogen cycling in an orchard ecosystem, *Sci. Total Environ.* 472 (2014) 939–946, <https://doi.org/10.1016/j.scitotenv.2013.11.117>. ISSN 0048-9697.
- [46] Francisco Alcon, Cristina Marín-Miñano, José A. Zabala, María-Dolores de-Miguel, José M. Martínez-Paz, Valuing diversification benefits through intercropping in Mediterranean agroecosystems: a choice experiment approach, *Ecol. Econ.* 171 (2020) 106593, <https://doi.org/10.1016/j.ecolecon.2020.106593>. ISSN 0921-8009.
- [47] Ding Wang, Wenbo Yi, Yanli Zhou, Shuran He, Li Tang, Xinhua Yin, Ping Zhao, Guangqiang Long, Intercropping and N application enhance soil dissolved organic carbon concentration with complicated chemical composition, *Soil Tillage Res.* 210 (2021) 104979, <https://doi.org/10.1016/j.still.2021.104979>. ISSN 0167-1987.
- [48] Simun Kolega, Begona Miras-Moreno, Valentina Buffagni, Luigi Lucini, Fabio Valentinuzzi, Mauro Maver, Tanja Mimmo, Marco Trevisan, Youry Pii, Stefano Cesco, Nutraceutical profiles of two hydroponically grown sweet basil cultivars as affected by the composition of the nutrient solution and the inoculation with *Azospirillum brasilense*, *Front. Plant Sci.* 11 (2020), <https://doi.org/10.3389/fpls.2020.596000>.
- [49] Parviz Rezvani Moghaddam, Rooholla Moradi, Hamed Mansoori, Influence of planting date, intercropping and plant growth promoting rhizobacteria on cumin (*Cuminum cyminum* L.) with particular respect to disease infestation in Iran, *Journal of Applied Research on Medicinal and Aromatic Plants* 1 (4) (2014) 134–143, <https://doi.org/10.1016/j.jarmap.2014.10.003>. ISSN 2214-7861.
- [50] Weria Weisany, Nawroz Abdul-razzak Tahir, Peer M. Schenk, Coriander/soybean intercropping and mycorrhizae application lead to overyielding and changes in essential oil profiles, *Eur. J. Agron.* 126 (2021) 126283, <https://doi.org/10.1016/j.eja.2021.126283>. ISSN 1161-0301.
- [51] R. Erfanzadeh, B. Bahrami, J. Motamedi, J. Pétilion, Changes in soil organic matter driven by shifts in co-dominant plant species in a grassland, *Geoderma* 213 (2014) 74–78, <https://doi.org/10.1016/j.geoderma.2013.07.027>.
- [52] Abhai Pratap Singh, Rashmi Singh, Usha Mina, Manesh Pratap Singh, Chandra Kumar Varshney, Emissions of monoterpene from tropical Indian plant species and assessment of VOCs emission from the forest of Haryana state, *Atmos. Pollut. Res.* 2 (1) (2011) 72–79, <https://doi.org/10.5094/APR.2011.009>. ISSN 1309-1042.

- [182] J. Gershenzon, N. Dudareva, The function of terpene natural products in the natural world, *Nat. Chem. Biol.* 3 (7) (2007) 408–414.
- [183] Zahra Bitarafan, Hamid Reza Asghari, Tahereh Hasanloo, Ahmad Gholami, Foad Moradi, Bekzod Khakimov, Fulai Liu, Christian Andreasen, The effect of charcoal on medicinal compounds of seeds of fenugreek (*Trigonella foenum-graecum* L.) exposed to drought stress, *Ind. Crop. Prod.* 131 (2019) 323–329, <https://doi.org/10.1016/j.indcrop.2019.02.003>. ISSN 0926-6690.
- [184] Christos N. Hassiotis, The role of aromatic *Salvia officinalis* L. on the development of two mycorrhizal fungi, *Biochem. Systemat. Ecol.* 77 (2018) 61–67, <https://doi.org/10.1016/j.bse.2018.01.004>. ISSN 0305-1978.
- [185] Luomeng Chao, Changwei Sun, Lihua Peng, Jiaxin Li, Sun Miao, Lihong Bao, Jia Liu, Yonghong Ma, Passive energy-saving buildings realized by the combination of transparent heat-shielding glass and energy storage cement, *Construct. Build. Mater.* 365 (2023) 130023, <https://doi.org/10.1016/j.conbuildmat.2022.130023>. ISSN 0950-0618.
- [186] C. Hemakumar, B.S. Ravindranath, G.A. Ravishankar, D.C. Ramirez, S.V. Kiran, Marmesin and marmelosin interact with the heparan sulfatase-2 active site: potential mechanism for phytochemicals from bael fruit extract as antitumor therapeutics, *Oxid. Med. Cell. Longev.* 2023 (2023 Jan 5) 9982194, <https://doi.org/10.1155/2023/9982194>. PMID: 36644581; PMCID: PMC9836799.
- [187] Florent Rossi, Raphaëlle Péguilhan, Nathalie Turgeon, Marc Veillette, Jean-Luc Baray, Laurent Deguillaume, Pierre Amato, Caroline Duchaine, Quantification of antibiotic resistance genes (ARGs) in clouds at a mountain site (puy de Dôme, central France), *Sci. Total Environ.* 865 (2023) 161264, <https://doi.org/10.1016/j.scitotenv.2022.161264>. ISSN 0048-9697.
- [188] J.L. Martínez, F. Baquero, Interactions among strategies associated with bacterial infection: pathogenicity, epidemicity, and antibiotic resistance, *Clin. Microbiol. Rev.* 15 (4) (2002 Oct) 647–679, <https://doi.org/10.1128/CMR.15.4.647-679.2002>. PMID: 12364374; PMCID: PMC126860.
- [189] M.H. Stockett, J.N. Bull, H. Cederquist, et al., Efficient stabilization of cyanonaphthalene by fast radiative cooling and implications for the resilience of small PAHs in interstellar clouds, *Nat. Commun.* 14 (2023) 395, <https://doi.org/10.1038/s41467-023-36092-0>.
- [190] A.K. Lemmens, D.B. Rap, J.M.M. Thunnissen, et al., Polycyclic aromatic hydrocarbon formation chemistry in a plasma jet revealed by IR-UV action spectroscopy, *Nat. Commun.* 11 (2020) 269, <https://doi.org/10.1038/s41467-019-14092-3>.
- [191] Xiaona Li, Shi Yao, Yongrong Bian, Xin Jiang, Yang Song, The combination of biochar and plant roots improves soil bacterial adaptation to PAH stress: insights from soil enzymes, microbiome, and metabolome, *J. Hazard Mater.* 400 (2020) 123227, <https://doi.org/10.1016/j.jhazmat.2020.123227>. ISSN 0304-3894.
- [192] A.V. Emeline, V.A. Otroshchenko, V.K. Ryabchuk, N. Serpone, Abiogenesis and photostimulated heterogeneous reactions in the interstellar medium and on primitive earth: relevance to the genesis of life, *J. Photochem. Photobiol. C Photochem. Rev.* 3 (3) (2003) 203–224, [https://doi.org/10.1016/S1389-5567\(02\)00039-4](https://doi.org/10.1016/S1389-5567(02)00039-4). ISSN 1389-5567.
- [193] Wendy L. Tate, Lydia Bals, Cristof Bals, Kai Foerstl, Seeing the forest and not the trees: learning from nature's circular economy, *Resour. Conserv. Recycl.* 149 (2019) 115–129, <https://doi.org/10.1016/j.resconrec.2019.05.023>. ISSN 0921-3449.